

Coalescence estimates for the corner growth model with exponential weights*

Timo Seppäläinen[†] Xiao Shen[‡]

Abstract

We establish estimates for the coalescence time of semi-infinite directed geodesics in the planar corner growth model with i.i.d. exponential weights. There are four estimates: upper and lower bounds on the probabilities of both fast and slow coalescence on the correct spatial scale with exponent $3/2$. Our proofs utilize a geodesic duality introduced by Pimentel and properties of the increment-stationary last-passage percolation process. For fast coalescence our bounds are new and they have matching optimal exponential order of magnitude. For slow coalescence we reproduce bounds proved earlier with integrable probability inputs, except that our upper bound misses the optimal order by a logarithmic factor.

Keywords: coalescence exit time; fluctuation exponent; geodesic; last-passage percolation; Kardar-Parisi-Zhang; random growth model.

AMS MSC 2010: 60K35; 60K37.

Submitted to EJP on November 27, 2019, final version accepted on June 27, 2020.

1 Introduction

Random growth models of the first- and last-passage type have been a central part of the mathematical theory of spatial stochastic processes since the seminal work of Eden [13] and Hammersley and Welsh [18]. In these models, growth proceeds along optimal paths called *geodesics*, determined by a random environment. The interesting and challenging objects of study are the *directed semi-infinite geodesics*. These pose an immediate existence question because they are asymptotic objects and hence cannot be defined locally in a simple manner. Once the existence question is resolved, questions concerning their multiplicity and geometric behavior such as coalescence arise.

Techniques for establishing the existence, uniqueness, and coalescence of semi-infinite geodesics were first introduced by Newman and co-authors in the 1990s [19,

*T. Seppäläinen was partially supported by National Science Foundation grants DMS-1602486 and DMS-1854619, and by the Wisconsin Alumni Research Foundation.

[†]University of Wisconsin–Madison. E-mail: seppalai@math.wisc.edu

[‡]University of Wisconsin–Madison. E-mail: xshen@math.wisc.edu

20, 22, 23] in the context of planar undirected first-passage percolation (FPP) with i.i.d. weights. These methods were subsequently applied to the exactly solvable planar directed last-passage percolation (LPP) model with i.i.d. exponential weights by Ferrari and Pimentel [16] and Coupier [12]. This model is also known as the exponential *corner growth model* (CGM).

A key technical point here is that the strict curvature hypotheses of Newman's work can be verified in the exactly solvable LPP model. A second key feature is that the exponential LPP model can be coupled with the totally asymmetric simple exclusion process (TASEP). This connection provides another suite of powerful tools for analyzing exponential LPP.

The work of [12] and [16] established for the exponential LPP model that, almost surely for a fixed direction, directed semi-infinite geodesics from each lattice point are unique and they coalesce. An alternative approach to these results was recently developed by one of the authors [28], by utilizing properties of the increment-stationary LPP process.

Once coalescence is known, attention turns to quantifying it: how fast do semi-infinite geodesics started from two distinct points coalesce? The scaling properties of planar models in the Kardar-Parisi-Zhang (KPZ) class come into the picture here. This class consists of interacting particle systems, random growth models and directed polymer models in two dimensions (one of which can be time) that share universal fluctuation exponents and limit distributions from random matrix theory. For surveys of the field, see [11, 25].

It is expected that, subject to mild moment assumptions on the weights, planar FPP and LPP are members of the KPZ class. It is conjectured in general and proved in exactly solvable cases that a geodesic of length N fluctuates on the scale $N^{2/3}$. Thus if two semi-infinite geodesics start at distance k apart, we expect coalescence to happen on the scale $k^{3/2}$.

The first step in the study of the coalescence exponent was taken by Wüthrich [29]. He proved a lower bound with exponent $3/2 - \epsilon$ for LPP on planar Poisson points. This was the first application of the first-passage percolation techniques of Newman and coauthors in the context of an exactly solvable last-passage percolation model. The second step in this direction was taken by Pimentel [24] for the exponential CGM. By relying on the TASEP connection, he proved that in a fixed direction, the so-called dual geodesic graph is equal in distribution (modulo a lattice reflection) to the original geodesic tree. Next, by appeal to fluctuation bounds derived by coupling techniques in [4], he derived an asymptotic lower bound on the coalescence time, with the expected exponent $3/2$.

The next step taken by Basu, Sarkar, and Sly [7] utilized the considerably more powerful estimates from integrable probability. For the upper bound on the coalescence time, they established not only the correct order of magnitude $k^{3/2}$ but also upper and lower probability bounds of matching orders of magnitude. In the same paper the original estimate of Pimentel was also improved significantly.

Our goal in taking up the speed of coalescence is the development of proof techniques that rely only on the stationary version of the model and avoid both the TASEP connection and integrable probability. The applicability of this approach then covers all $1+1$ dimensional KPZ models with a tractable stationary version. This includes not only various last-passage models in both discrete and continuous space, but also the four currently known solvable positive temperature polymer models [10]. Extension beyond solvable models may also be possible, as indicated by the exact KPZ fluctuation exponents derived in [5] for a class of zero-range processes outside currently known exactly solvable models. This is work left for the future. Another somewhat philosophical point is that

capturing exponents should be possible without integrable probability. This has been demonstrated for fluctuation exponents by [4] for the exponential LPP and by [26] for a positive-temperature directed polymer model.

The results of this paper come from a unified approach based on controlling the exit point of the geodesic in a stationary LPP process and on Pimentel's duality of geodesics and dual geodesics. This involves coupling, random walk estimates, planar monotonicity, and distributional properties of the stationary LPP process. Here are the precise contributions of the present paper (details in Section 2.2):

- (i) The upper and lower bounds for slow coalescence originally due to Basu et al. [7], though our upper bound falls short of the optimal order by a logarithmic factor (Theorem 2.2). Our contribution here is to give a proof without integrable probability inputs.
- (ii) Upper and lower bounds for fast coalescence of matching exponential order (Theorem 2.3). These are new results.
- (iii) A lower bound on the transversal fluctuations of a directed semi-infinite geodesic which improves bounds obtainable without integrable probability (Theorem 2.8).
- (iv) Strengthened exit time estimates for the stationary LPP process without integrable probability, some uniform over endpoints beyond a given distance (Theorems 4.1, 4.4, 4.5).

We mention two more general but related points about the exponential CGM.

(a) When all directions are considered simultaneously, the overall picture of semi-infinite geodesics is richer than the simple almost-sure-uniqueness-plus-coalescence valid for a fixed direction. Part of this was already explained by Coupier [12]. Recently the global picture of uniqueness and coalescence was captured in [21]. Coalescence bounds that go beyond the almost surely unique geodesics in a fixed direction are left as an open problem for the future.

(b) Various geometric features of the exponential LPP process can now be proved without appeal to properties of TASEP. An exception is a deep result of Coupier [12] on the absence of triple geodesics in any random direction. This fact currently has no proof except the original one that relies on the *TASEP speed process* introduced in [1].

Organization of the paper

Precise definition of the exponential LPP model and the main results appear in Section 2. Section 3 collects known facts about the CGM used in the proofs. This includes properties of the stationary growth process and the construction of the directed semi-infinite geodesics in terms of Busemann functions. Section 4 derives new exit time estimates for the geodesic of the stationary growth process, stated as Theorems 4.1, 4.4, and 4.5. In the final Section 5 the exit time estimates and duality are combined to prove the main results of Section 2. The appendix contains a random walk estimate and a moment bound on the Radon-Nikodym derivative between two product-form exponential distributions.

Notation and conventions

Points $x = (x_1, x_2), y = (y_1, y_2) \in \mathbb{R}^2$ are ordered coordinatewise: $x \leq y$ iff $x_1 \leq y_1$ and $x_2 \leq y_2$. The ℓ^1 norm is $|x|_1 = |x_1| + |x_2|$. The origin of \mathbb{R}^2 is denoted by both 0 and $(0, 0)$. The two standard basis vectors are $e_1 = (1, 0)$ and $e_2 = (0, 1)$. For $a \leq b$ in \mathbb{Z}^2 , $\llbracket a, b \rrbracket = \{x \in \mathbb{Z}^2 : a \leq x \leq b\}$ is the rectangle in \mathbb{Z}^2 with corners a and b . $\llbracket a, b \rrbracket$ is a segment if a and b are on the same horizontal or vertical line. We use $\llbracket a - e_1, a \rrbracket, \llbracket a - e_2, a \rrbracket$

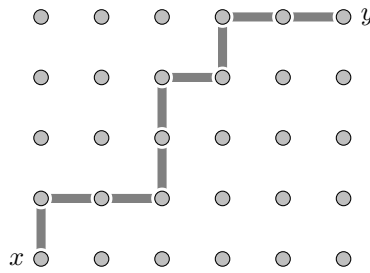


Figure 2.1: An up-right path between two integer points x and y .

to denote unit edges when it is clear from the context. Subscripts indicate restricted subsets of the reals and integers: for example $\mathbb{Z}_{>0} = \{1, 2, 3, \dots\}$ and $\mathbb{Z}_{>0}^2 = (\mathbb{Z}_{>0})^2$ is the positive first quadrant of the planar integer lattice. For $0 < \alpha < \infty$, $X \sim \text{Exp}(\alpha)$ means that the random variable X has exponential distribution with rate α , in other words $P(X > t) = e^{-\alpha t}$ for $t > 0$ and $E(X) = \alpha^{-1}$.

2 Main results

2.1 The corner growth model and semi-infinite geodesics

The *standard exponential corner growth model* (CGM) is defined on the planar integer lattice \mathbb{Z}^2 through independent and identically distributed (i.i.d.) weights $\{\omega_z\}_{z \in \mathbb{Z}^2}$, indexed by the vertices of \mathbb{Z}^2 , with marginal distribution $\omega_z \sim \text{Exp}(1)$. The *last-passage value* $G_{x,y}$ between two coordinatewise-ordered vertices $x \leq y$ of \mathbb{Z}^2 is the maximal total weight of an up-right nearest-neighbor path from x to y :

$$G_{x,y} = \max_{z \in \Pi^{x,y}} \sum_{k=0}^{|y-x|_1} \omega_{z_k} \tag{2.1}$$

where $\Pi^{x,y}$ is the set of paths $z_\cdot = (z_k)_{k=0}^{|y-x|_1}$ that satisfy $z_0 = x$, $z_{|y-x|_1} = y$, and $z_{k+1} - z_k \in \{e_1, e_2\}$. The almost surely unique maximizing path is the *point-to-point geodesic*. $G_{x,y}$ is also called (directed) *last-passage percolation* (LPP). If $x \leq y$ fails our convention is $G_{x,y} = -\infty$.

A semi-infinite up-right path $(z_i)_{i=0}^\infty$ is a *semi-infinite geodesic* if it is the maximizing path between any two points on this path, that is,

$$\forall k < l \text{ in } \mathbb{Z}_{\geq 0} : (z_i)_{i=k}^l \in \Pi^{z_k, z_l} \quad \text{and} \quad G_{z_k, z_l} = \sum_{i=k}^l \omega_{z_i}.$$

For a point $\xi \in \mathbb{R}_{\geq 0}^2 \setminus \{0\}$, the semi-infinite path $(z_i)_{i=0}^\infty$ is ξ -*directed* if $z_i / |z_i|_1 \rightarrow \xi / |\xi|_1$ as $i \rightarrow \infty$.

In the exponential CGM it is natural to index spatial directions ξ by a real parameter $\rho \in (0, 1)$ through the equation

$$\xi[\rho] = ((1 - \rho)^2, \rho^2). \tag{2.2}$$

We call $\xi[\rho]$ the *characteristic direction* associated to parameter ρ . This notion acquires meaning when we discuss the stationary LPP process in Section 3. Throughout, N will be a scaling parameter that goes to infinity. When ρ is understood, we write

$$v_N = (\lfloor N(1 - \rho)^2 \rfloor, \lfloor N\rho^2 \rfloor) \tag{2.3}$$

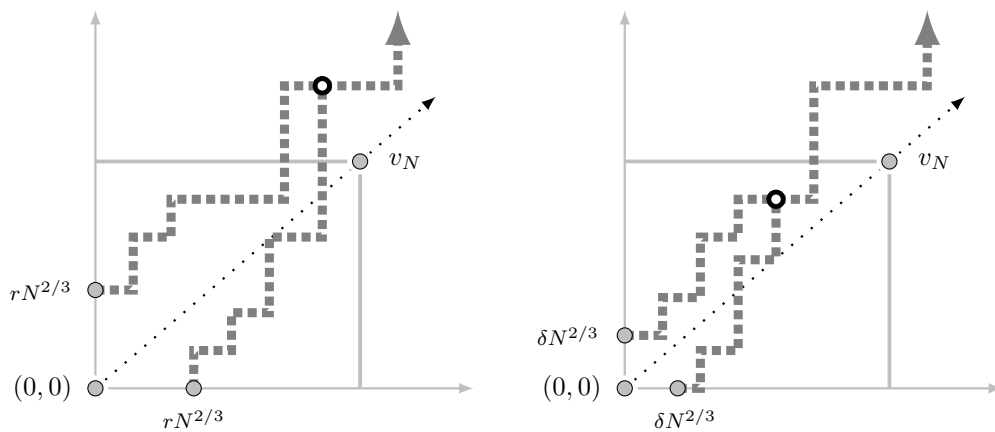


Figure 2.2: Coalescence of $\xi[\rho]$ -directed semi-infinite geodesics. The black circle marks the coalescence point: on the left it is $\mathbf{z}^\rho(\lfloor rN^{2/3} \rfloor e_1, \lfloor rN^{2/3} \rfloor e_2)$, and on the right $\mathbf{z}^\rho(\lfloor \delta N^{2/3} \rfloor e_1, \lfloor \delta N^{2/3} \rfloor e_2)$. On the left for large r the geodesics are likely to coalesce outside the rectangle $\llbracket 0, v_N \rrbracket$, while on the right for small δ the geodesics are likely to coalesce inside the rectangle $\llbracket 0, v_N \rrbracket$.

for the lattice point moving in direction $\xi[\rho]$.

The theorem below summarizes the key facts about directed semi-infinite geodesics that set the stage for our paper. It goes back to the work of Ferrari and Pimentel [16] and Coupier [12] on the CGM, and the general geodesic techniques introduced by Newman and coworkers [19, 20, 22, 23]. A different proof is given in [28].

Theorem 2.1. Fix $\rho \in (0, 1)$. Then the following holds almost surely. For each $x \in \mathbb{Z}^2$ there is a unique $\xi[\rho]$ -directed semi-infinite geodesic $\mathbf{b}^{\rho,x} = (\mathbf{b}_i^{\rho,x})_{i=0}^\infty$ such that $\mathbf{b}_0^{\rho,x} = x$. For each pair $x, y \in \mathbb{Z}^2$, the geodesics coalesce: there is a coalescence point $\mathbf{z}^\rho(x, y)$ such that $\mathbf{b}^{\rho,x} \cap \mathbf{b}^{\rho,y} = \mathbf{b}^{\rho,z}$ for $z = \mathbf{z}^\rho(x, y)$.

2.2 Coalescence estimates for semi-infinite geodesics in a fixed direction

The two main results below give upper and lower bounds on the probability that two $\xi[\rho]$ -directed semi-infinite geodesics initially separated by a distance of order $N^{2/3}$ coalesce inside the rectangle $\llbracket 0, v_N \rrbracket$. The theorems are separated according to whether the starting points of the geodesics are close to each other or far apart on the scale $N^{2/3}$. See the illustration in Figure 2.2. As introduced in Theorem 2.1, $\mathbf{z}^\rho(x, y)$ is the coalescence point of the geodesics $\mathbf{b}^{\rho,x}$ and $\mathbf{b}^{\rho,y}$.

Theorem 2.2. For each $0 < \rho < 1$ there exist finite positive constants δ_0, C_1, C_2 and N_0 that depend only on ρ and for which the following holds: whenever $N \geq N_0$ and $N^{-2/3} \leq \delta \leq \delta_0$,

$$C_1 \delta \leq \mathbb{P}\{\mathbf{z}^\rho(\lfloor \delta N^{2/3} \rfloor e_1, \lfloor \delta N^{2/3} \rfloor e_2) \notin \llbracket 0, v_N \rrbracket\} \leq C_2 |\log \delta|^{2/3} \delta. \tag{2.4}$$

The requirement $\delta \geq N^{-2/3}$ in Theorem 2.2 is needed only for the lower bound and only to ensure that $\lfloor \delta N^{2/3} \rfloor \neq 0$.

Theorem 2.3. For each $0 < \rho < 1$ there exist finite positive constants r_0, C_1, C_2 and N_0 that depend only on ρ and for which the following holds: whenever $N \geq N_0$ and

$$r_0 \leq r \leq ((1 - \rho)^2 \wedge \rho^2)N^{1/3},$$

$$e^{-C_1 r^3} \leq \mathbb{P}\{\mathbf{z}^\rho(\lfloor rN^{2/3} \rfloor e_1, \lfloor rN^{2/3} \rfloor e_2) \in \llbracket 0, v_N \rrbracket\} \leq e^{-C_2 r^3}. \tag{2.5}$$

The requirement $r \leq ((1 - \rho)^2 \wedge \rho^2)N^{1/3}$ in Theorem 2.3 is needed only for the lower bound and only to ensure that both geodesics start inside the rectangle $\llbracket 0, v_N \rrbracket$.

If we replace one of the starting points with the origin 0, the upper bound of Theorem 2.2 and the lower bound of Theorem 2.3 hold automatically because $\mathbf{b}^{\rho,0}$ stays between $\mathbf{b}^{\rho,(\lfloor rN^{2/3} \rfloor,0)}$ and $\mathbf{b}^{\rho,(0,\lfloor rN^{2/3} \rfloor)}$. The following corollary states that the other two tail estimates also hold with possibly different constants under this alteration in the geometry.

Corollary 2.4. *For each $0 < \rho < 1$ there exist finite positive constants δ_0, r_0, C_1, C_2 and N_0 that depend only on ρ and for which the following holds: whenever $N \geq N_0$, $N^{-2/3} \leq \delta \leq \delta_0$, and $r \geq r_0$,*

(i) $\mathbb{P}\{\mathbf{z}^\rho(0, \lfloor \delta N^{2/3} \rfloor e_1) \notin \llbracket 0, v_N \rrbracket\} \geq C_1 \delta$ and

(ii) $\mathbb{P}\{\mathbf{z}^\rho(0, \lfloor rN^{2/3} \rfloor e_1) \in \llbracket 0, v_N \rrbracket\} \leq e^{-C_2 r^3}$.

Remark 2.5. Two comments about the results.

(a) The statements of the theorems are valid for $v_N = (\lfloor Na \rfloor, \lfloor Nb \rfloor)$ for any fixed $a, b > 0$, with new constants that depend also on a, b . The characteristic point v_N of (2.3) is simply one natural choice.

(b) The constants in the theorems that depend on $\rho \in (0, 1)$ can be taken fixed uniformly for all ρ in any compact subset of $(0, 1)$.

For direct comparison with [7], we state two corollaries for geodesics whose locations are not expressed in terms of the large parameter N .

Corollary 2.6. *For each $0 < \rho < 1$ there exist finite positive constants R_0, C_1 and C_2 that depend only on ρ and for which the following holds: whenever $k \geq 1$ and $R \geq R_0$,*

$$C_1 R^{-2/3} \leq \mathbb{P}\{\mathbf{z}^\rho(\lfloor k^{2/3} \rfloor e_1, \lfloor k^{2/3} \rfloor e_2) \notin \llbracket 0, v_{Rk} \rrbracket\} \leq C_2 (\log R)^{2/3} R^{-2/3}. \tag{2.6}$$

Corollary 2.6 is derived from Theorem 2.2 as follows. Set $R_0 = N_0 \vee \delta_0^{-3/2}$. Given $k \geq 1$ and $R \geq R_0$, let $N = Rk \geq N_0$ and $\delta = R^{-2/3} \leq \delta_0$. Now $k^{2/3} = \delta N^{2/3}$. The next Corollary 2.7 below is derived from Theorem 2.3 in a similar way.

Corollary 2.7. *For each $0 < \rho < 1$ there exist finite positive constants R_1, C_1 and C_2 that depend only on ρ and for which the following holds: whenever $k \geq 1$ and $((1 - \rho)^2 \wedge \rho^2)^{-1} k^{-1/3} \leq R \leq R_1$,*

$$e^{-C_1 R^{-2}} \leq \mathbb{P}\{\mathbf{z}^\rho(\lfloor k^{2/3} \rfloor e_1, \lfloor k^{2/3} \rfloor e_2) \in \llbracket 0, v_{Rk} \rrbracket\} \leq e^{-C_2 R^{-2}}. \tag{2.7}$$

Again, the lower bound $R \geq ((1 - \rho)^2 \wedge \rho^2)^{-1} k^{-1/3}$ is imposed only to ensure that both geodesics start inside the rectangle $\llbracket 0, v_{Rk} \rrbracket$, for otherwise the probability in Corollary 2.7 is zero.

The lower bounds in Theorem 2.2 and Corollary 2.6 are optimal, but the upper bounds are not due to the logarithmic factor. Optimal upper and lower bounds (both of order $R^{-2/3}$) were proved for Corollary 2.6 by Basu, Sarkar, and Sly [7] with inputs from integrable probability. Thus in Theorem 2.2 and Corollary 2.6 our contribution is to provide bounds without relying on integrable probability.

Both upper and lower bounds in Theorem 2.3 are new. The upper bound $e^{-C_2 r^3}$ of Theorem 2.3 improves significantly Pimentel’s [24] asymptotic ($N \rightarrow \infty$) upper bound $C r^{-3}$. The improved bound comes from duality and an exit time estimate with the

optimal exponential order, obtained recently by Emrah, Janjigian, and one of the authors in [14] without integrable probability inputs. This exit time estimate was also derived independently by Bhatia [8] with integrable probability inputs. In the intervening period between Pimentel’s work and the present paper, Pimentel’s bound was improved to $e^{-Cr^{3/2}}$ (without sending N to infinity) in [7] with inputs from integrable probability, see [7, Remark 6.5].

It is by now well-known that over distances of order N , geodesics fluctuate on the scale $N^{2/3}$. A by-product of our proof is the following lower bound on the size of the transversal fluctuation of a semi-infinite geodesic. It is an improvement over previous bounds obtained without integrable probability (see Theorem 5.3(b) in [27]).

Theorem 2.8. *For each $0 < \rho < 1$ there exist positive constants C , N_0 and δ_0 that depend only on ρ for which the following holds: whenever $N \geq N_0$ and $0 < \delta \leq \delta_0$,*

$$\mathbb{P}\{\mathbf{b}^{\rho,(0,0)} \text{ enters the rectangle } \llbracket v_N - \delta N^{2/3}(e_1 + e_2), v_N \rrbracket\} \leq C|\log \delta|^{2/3}\delta. \quad (2.8)$$

The proofs in Section 5 show that the probability in (2.8) is essentially bounded above by the probability in (2.4). With inputs from integrable probability, the upper bound $|\log \delta|^{2/3}\delta$ in (2.8) can be improved to δ , the optimal upper bound for (2.4) obtained in [7].

We turn to develop the groundwork for the proofs.

3 Preliminaries on the corner growth model

This section covers aspects of the CGM used in the proofs. We provide illustrations, some intuitive arguments, and references to precise proofs. The two main results are a fluctuation upper bound for the exit point of a stationary LPP process (Theorem 3.5) and the construction of semi-infinite geodesics with Busemann functions (Theorem 3.7). These are proved in article [14] and lecture notes [27], without using anything beyond the stationary LPP process.

3.1 Nonrandom properties

We begin with two basic features of LPP that involve increments. We state them for our exponential case but in fact these properties do not need any probability. Let $G_{x,\cdot}$ be defined by (2.1) and define increment variables for $a \geq x + e_1$ and $b \geq x + e_2$ by

$$I_a^x = G_{x,a} - G_{x,a-e_1} \quad \text{and} \quad J_b^x = G_{x,b} - G_{x,b-e_2}.$$

The first property is a monotonicity valid for planar LPP. Proof can be found for example in Lemma 4.6 of [27].

Lemma 3.1. *For y such that the increments are well-defined,*

$$I_y^{x-e_1} \leq I_y^x \leq I_y^{x-e_2} \quad \text{and} \quad J_y^{x-e_2} \leq J_y^x \leq J_y^{x-e_1}.$$

Fix distinct lattice points $x \leq z$ and define a second LPP process $G_{z,\cdot}^{(x)}$ with base point at z that uses boundary weights given by the increments of $G_{x,\cdot}$, as illustrated in Figure 3.1. Precisely, for $y \geq z$,

$$G_{z,y}^{(x)} = \max_{z \in \Pi^{z,y}} \sum_{k=0}^{|y-z|_1} \eta_{z_k} \quad (3.1)$$

where the weights are given by

$$\begin{aligned} \eta_z &= 0, & \eta_a &= \omega_a \quad \text{for } a \in z + \mathbb{Z}_{>0}^2 \text{ (bulk),} \\ \eta_{z+ke_1} &= I_{z+ke_1}^x, & \eta_{z+ke_2} &= J_{z+ke_2}^x \quad \text{for } k \geq 1 \text{ (boundary).} \end{aligned} \quad (3.2)$$

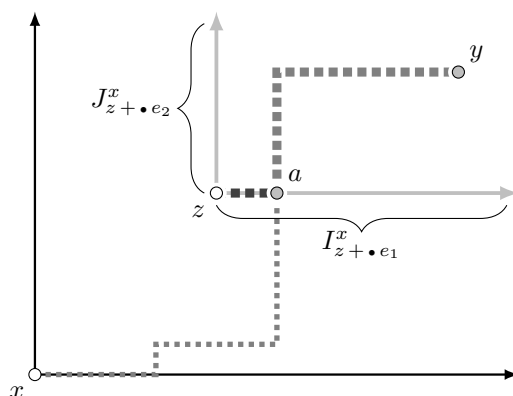


Figure 3.1: Illustration of Lemma 3.2. LPP process $G_{z,\bullet}^{(x)}$ uses boundary weights defined by the LPP process $G_{x,\bullet}$. Path x - a - y is the geodesic of $G_{x,y}$ and path z - a - y the geodesic of $G_{z,y}^{(x)}$. These geodesics share the segment a - y .

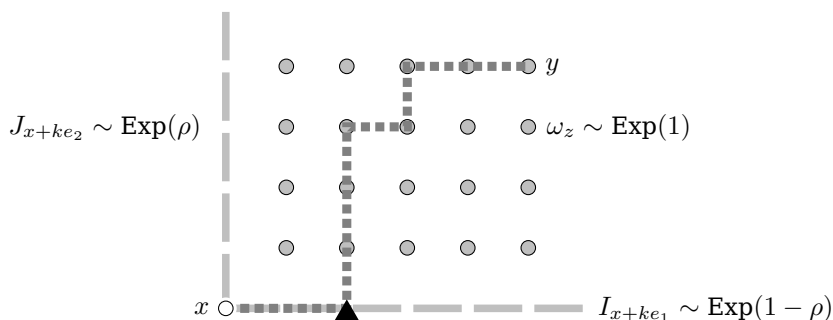


Figure 3.2: Increment-stationary LPP with base point x . If the dotted line were the geodesic of $G_{x,y}^\rho$, then the black triangle highlights the exit point, and the exit time is $\mathbf{Z}^{x \rightarrow y} = 2$.

Proof of the lemma below is elementary and can be found in Lemma A.1 of [27].

Lemma 3.2. *Let $x \leq z$ and $y \in z + \mathbb{Z}_{>0}^2$. Then the unique geodesics of $G_{x,y}$ and $G_{z,y}^{(x)}$ coincide in the quadrant $z + \mathbb{Z}_{>0}^2$.*

3.2 Stationary last-passage percolation

The stationary LPP process G^ρ is defined on a positive quadrant $x + \mathbb{Z}_{\geq 0}^2$ with a fixed base point $x \in \mathbb{Z}^2$. It is parametrized by $\rho \in (0, 1)$. Start with mutually independent bulk weights $\{\omega_z : z \in x + \mathbb{Z}_{>0}^2\}$ and boundary weights $\{I_{x+ke_1}, J_{x+le_2} : k, l \in \mathbb{Z}_{>0}\}$ with marginal distributions

$$\omega_z \sim \text{Exp}(1), \quad I_{x+ke_1} \sim \text{Exp}(1 - \rho), \quad \text{and} \quad J_{x+le_2} \sim \text{Exp}(\rho). \quad (3.3)$$

The probability distribution of these weights is denoted by \mathbb{P}^ρ . The LPP process $G_{x,\bullet}^\rho$ is defined on the boundary of the quadrant by $G_{x,x}^\rho = 0$, $G_{x,x+ke_1}^\rho = \sum_{i=1}^k I_{x+ie_1}$ and $G_{x,x+le_2}^\rho = \sum_{j=1}^l J_{x+je_2}$ for $k, l \geq 1$. In the bulk we perform LPP that uses both the

boundary and the bulk weights: for $y = x + (m, n) \in x + \mathbb{Z}_{>0}^2$,

$$G_{x,y}^\rho = \max_{1 \leq k \leq m} \left\{ \left(\sum_{i=1}^k I_{x+ie_1} \right) + G_{x+ke_1+e_2,y} \right\} \vee \max_{1 \leq l \leq n} \left\{ \left(\sum_{j=1}^l J_{x+je_2} \right) + G_{x+le_2+e_1,y} \right\}. \tag{3.4}$$

The LPP value $G_{a,b}$ inside the braces is the standard one defined by (2.1) with the i.i.d. bulk weights ω . Call the almost surely unique maximizing path a ρ -geodesic. The exit time $\mathbf{Z}^{x \rightarrow y}$ is the $\mathbb{Z} \setminus \{0\}$ -valued random variable that records where the ρ -geodesic from x to y exits the boundary, relative to the base point x , with a sign that indicates choice between the axes:

$$G_{x,y}^\rho = \begin{cases} \sum_{i=1}^k I_{x+ie_1} + G_{x+ke_1+e_2,y}, & \text{if } \mathbf{Z}^{x \rightarrow y} = k > 0 \\ \sum_{j=1}^l J_{x+je_2} + G_{x+le_2+e_1,y}, & \text{if } \mathbf{Z}^{x \rightarrow y} = -l < 0. \end{cases} \tag{3.5}$$

See Figure 3.2 for an illustration.

Define horizontal and vertical increments of $G_{x,\cdot}^\rho$, as

$$I_a^x = G_{x,a}^\rho - G_{x,a-e_1}^\rho \quad \text{and} \quad J_b^x = G_{x,b}^\rho - G_{x,b-e_2}^\rho \tag{3.6}$$

for $a \in x + \mathbb{Z}_{>0} \times \mathbb{Z}_{\geq 0}$ and $b \in x + \mathbb{Z}_{\geq 0}^2 \times \mathbb{Z}_{>0}$. The definition above implies $I_{ke_1}^x = I_{ke_1}$ and $J_{le_2}^x = J_{le_2}$ for $k, l \geq 1$. The term (increment) stationary LPP is justified by the next fact. Its proof is an induction argument and can be found for example in [27, Thm. 3.1].

Lemma 3.3. *Let $\{y_i\}$ be any finite or infinite down-right path in $x + \mathbb{Z}_{\geq 0}^2$. That is, $(y_{i+1} - y_i) \cdot e_2 \leq 0 \leq (y_{i+1} - y_i) \cdot e_1$. Then the increments $\{G_{x,y_{i+1}}^\rho - G_{x,y_i}^\rho\}$ are independent. The marginal distributions of nearest-neighbor increments are $I_a^x \sim \text{Exp}(1 - \rho)$ and $J_b^x \sim \text{Exp}(\rho)$.*

Now apply Lemma 3.2 to this stationary situation. Take $z \in x + \mathbb{Z}_{\geq 0}^2$ and define the LPP process $G_{z,\cdot}^{(x),\rho}$ with the recipe (3.1) where the boundary weights are the ones in (3.6). By Lemma 3.3, these boundary weights have the same distribution as the original ones in (3.3). Consequently $G_{z,\cdot}^{(x),\rho}$ is another stationary LPP process. Lemma 3.2 gives the statement below which will be used extensively in our proofs.

Lemma 3.4. *Let $x \leq z$ and $y \in z + \mathbb{Z}_{>0}^2$. Then the unique geodesics of $G_{x,y}^\rho$ and $G_{z,y}^{(x),\rho}$ coincide in the quadrant $z + \mathbb{Z}_{>0}^2$.*

Since the boundary weights in (3.3) are stochastically larger than the bulk weights, the ρ -geodesic prefers the boundaries. The characteristic direction $\xi[\rho] = ((1 - \rho)^2, \rho^2)$ defined earlier in (2.2) is the unique direction in which the attraction of the e_1 - and e_2 -axes balance each other out. A consequence of this is that the ρ -geodesic from x to $x + v_N$ spends order $N^{2/3}$ steps on the boundary. Here we encounter the $2/3$ wandering exponent of KPZ universality. This is described in Theorems 3.5 and 4.5 below. The macroscopic picture is in Figure 3.3. This matter is discussed more thoroughly in Section 3.2 of [27]. We record the upper bound for this exit time recently derived in [14].

Theorem 3.5. [14, Theorem 2.5] *There exist positive constants r_0, N_0, C that depend only on ρ such that for all $r > r_0, N \geq N_0$, and $|v - v_N|_1 \leq N^{2/3}$,*

$$\mathbb{P}^\rho \{ |\mathbf{Z}^{0 \rightarrow v}| \geq rN^{2/3} \} \leq e^{-Cr^3}.$$

In the next corollary the $\Theta(N^{2/3})$ deviation is transferred from the base point 0 to the endpoint v_N . Figure 3.4 illustrates how Lemma 3.4 reduces claim (3.8) to Theorem 3.5. (Corollary 3.6 is proved using the same method as Corollary 5.10 in the arXiv version of [27].)

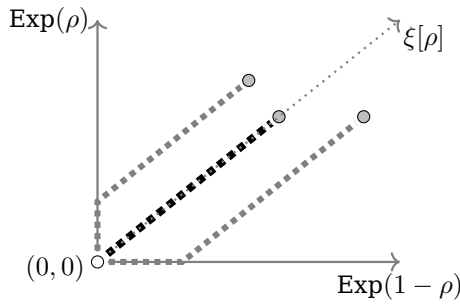


Figure 3.3: A macroscopic view of point-to-point geodesics (dotted lines) in stationary LPP from the base point at the origin $(0, 0)$ to three different endpoints (gray bullets). Only the geodesic in the characteristic direction $\xi[\rho]$ spends no macroscopic time on the boundary.

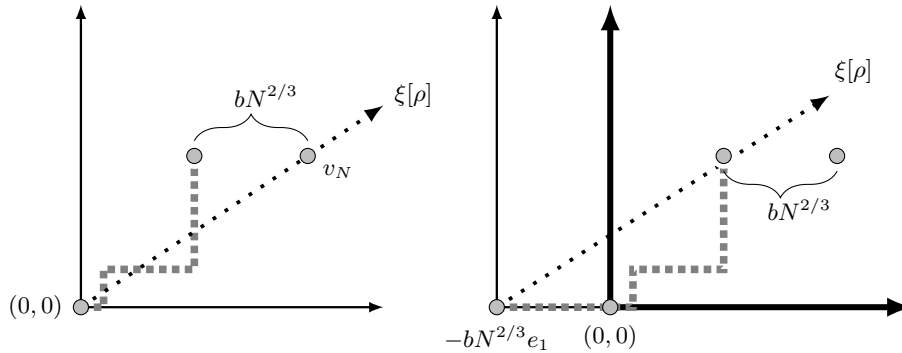


Figure 3.4: Proof of (3.8). On the left the event $\mathbf{Z}^0 \rightarrow v_N - [bN^{2/3}]e_1 \geq 1$. On the right a second base point is placed at $-[bN^{2/3}]e_1$ and the increment variables on the e_2 -axis based at 0 are determined by the LPP process based at $-[bN^{2/3}]e_1$. By Lemma 3.4, $\mathbf{Z}^0 \rightarrow v_N - [bN^{2/3}]e_1 \geq 1$ iff $\mathbf{Z}^{-[bN^{2/3}]e_1} \rightarrow v_N - [bN^{2/3}]e_1 \geq bN^{2/3}$. This last event has probability $\leq e^{-Cb^{-3}}$ by Theorem 3.5.

Corollary 3.6. *There exist positive constants N_0, C that depend only on ρ such that for $N \geq N_0$ and $b > 0$,*

$$\mathbb{P}^\rho \{ \mathbf{Z}^0 \rightarrow v_N + [bN^{2/3}]e_1 \leq -1 \} \leq e^{-Cb^3} \quad \text{and} \quad (3.7)$$

$$\mathbb{P}^\rho \{ \mathbf{Z}^0 \rightarrow v_N - [bN^{2/3}]e_1 \geq 1 \} \leq e^{-Cb^3}. \quad (3.8)$$

3.3 Busemann functions and semi-infinite geodesics

The key to our results is that the directed semi-infinite geodesics can be defined through Busemann functions, which themselves are instances of stationary LPP. Thus estimates proved for stationary LPP provide information about the behavior of directed semi-infinite geodesics.

The next theorem summarizes the properties of Busemann functions needed. It is a combination of results from Section 4 of [27] and Lemma 4.1 of [28]. The dual weights introduced in part (iii) below are connected with *dual geodesics* which will be constructed later in Section 5.

Theorem 3.7. Fix $\rho \in (0, 1)$. Then on the probability space of the i.i.d. $\text{Exp}(1)$ weights $\{\omega_z\}_{z \in \mathbb{Z}^2}$ there exists a process $\{B_{x,y}^\rho\}_{x,y \in \mathbb{Z}^2}$ with the following properties.

(i) With probability one, $\forall x, y \in \mathbb{Z}^2$,

$$B_{x,y}^\rho = \lim_{N \rightarrow \infty} (G_{x,u_N} - G_{y,u_N})$$

for any sequence u_N such that $|u_N| \rightarrow \infty$ and $u_N/|u_N|_1 \rightarrow \xi[\rho]/|\xi[\rho]|_1$ as $N \rightarrow \infty$.

(ii) The unique $\xi[\rho]$ -directed semi-infinite geodesic from x is defined by $\mathbf{b}_0^{\rho,x} = x$ and for $k \geq 0$,

$$\mathbf{b}_{k+1}^{\rho,x} = \begin{cases} \mathbf{b}_k^{\rho,x} + e_1, & \text{if } B_{\mathbf{b}_k^{\rho,x}, \mathbf{b}_k^{\rho,x} + e_1}^\rho \leq B_{\mathbf{b}_k^{\rho,x}, \mathbf{b}_k^{\rho,x} + e_2}^\rho \\ \mathbf{b}_k^{\rho,x} + e_2, & \text{if } B_{\mathbf{b}_k^{\rho,x}, \mathbf{b}_k^{\rho,x} + e_2}^\rho < B_{\mathbf{b}_k^{\rho,x}, \mathbf{b}_k^{\rho,x} + e_1}^\rho. \end{cases} \quad (3.9)$$

(iii) Define the dual weights by

$$\check{\omega}_z^\rho = B_{z-e_1,z}^\rho \wedge B_{z-e_2,z}^\rho \quad \text{for } z \in \mathbb{Z}^2.$$

Fix a bi-infinite nearest-neighbor down-right path $\gamma = \{x_i\}_{i \in \mathbb{Z}}$ on \mathbb{Z}^2 . This means that $x_{i+1} - x_i \in \{e_1, -e_2\}$. Then the random variables

$$\{B_{x_i, x_{i+1}}^\rho : i \in \mathbb{Z}\}, \{\omega_y : y \in \mathbb{Z}^2 \text{ lies strictly to the left of and below } \gamma\},$$

and $\{\check{\omega}_z^\rho : z \in \mathbb{Z}^2 \text{ lies strictly to the right of and above } \gamma\}$

are all mutually independent with marginal distributions

$$B_{x, x+e_1}^\rho \sim \text{Exp}(1 - \rho), \quad B_{x, x+e_2}^\rho \sim \text{Exp}(\rho) \quad \text{and} \quad \omega_y, \check{\omega}_z^\rho \sim \text{Exp}(1). \quad (3.10)$$

Versions of parts (i) and (ii) above can be proved for general i.i.d. weights [17]. But nothing like part (iii) with precise distributions for Busemann functions and dual weights is known for LPP models that are not exactly solvable.

A Busemann function B^ρ can be thought as a stationary LPP process in two ways. One with north and east boundaries, denoted by $G^{\rho, NE}$, and one with south and west boundaries, denoted by G^ρ . Here G^ρ is as was given in (3.4), and $G^{\rho, NE}$ is defined as follows (NE stands for north and east boundaries).

Fix an origin or base point $x \in \mathbb{Z}^2$. Start with mutually independent bulk weights $\{\omega_z : z \in x - \mathbb{Z}_{>0}^2\}$ and boundary weights $\{I_{x-ke_1}, J_{x-le_2} : k, l \in \mathbb{Z}_{\geq 0}\}$ with marginal distributions

$$\omega_z \sim \text{Exp}(1), \quad I_{x-ke_1} \sim \text{Exp}(1 - \rho), \quad \text{and} \quad J_{x-le_2} \sim \text{Exp}(\rho).$$

On the boundaries define $G_{x,x}^{NE,\rho} = 0$, $G_{x-ke_1,x}^{NE,\rho} = \sum_{i=0}^{k-1} I_{x-ie_1}$ and $G_{x+le_2,x}^{NE,\rho} = \sum_{j=0}^{l-1} J_{x-je_2}$ for $k, l \geq 1$. In the bulk we perform LPP that uses both the boundary and the bulk weights: for $y = x - (m, n) \in x - \mathbb{Z}_{>0}^2$,

$$G_{y,x}^{NE,\rho} = \max_{1 \leq k \leq m} \left\{ \left(\sum_{i=0}^{k-1} I_{x-ie_1} \right) + G_{y, x-ke_1-e_2} \right\} \vee \max_{1 \leq l \leq n} \left\{ \left(\sum_{j=0}^{l-1} J_{x-je_2} \right) + G_{y, x-le_2-e_1} \right\}. \quad (3.11)$$

The LPP value $G_{a,b}$ inside the braces is the one defined by (2.1) with i.i.d. bulk weights ω .

Two stationary LPP processes can be defined by taking Busemann increments as boundary weights. Fix again a base point $x \in \mathbb{Z}^2$.

- Construct $G_{y,x}^{\rho,NE}$ for $y \leq x$ as in (3.11) using the NE boundary weights $I_{x-ke_1} = B_{x-(k+1)e_1, x-ke_1}^\rho$ and $J_{x-le_2} = B_{x-(l+1)e_2, x-le_2}^\rho$ and bulk weights $\{\omega_z : z \in x - \mathbb{Z}_{>0}^2\}$.
- Construct $G_{x,y'}^\rho$ for $y' \geq x$ as in (3.4) using the SW boundary weights $I_{x+ke_1} = B_{x+(k-1)e_1, x+ke_1}^\rho$ and $J_{x+le_2} = B_{x+(l-1)e_2, x+le_2}^\rho$ and bulk weights $\{\check{\omega}_z : z \in x + \mathbb{Z}_{>0}^2\}$.

These two constructions satisfy the definitions of stationary LPP processes due to Theorem 3.7(iii). Their key properties relative to the Busemann function are

$$G_{y,x}^{\rho,NE} = B_{y,x}^\rho \quad \text{for all } y \leq x \tag{3.12}$$

$$\text{and } G_{x,y'}^\rho = B_{x,y'}^\rho \quad \text{for all } y' \geq x. \tag{3.13}$$

This is in Theorem 4.4 of [27].

As the last point, we state an independence property for a coupling of Busemann functions in two different directions. This fact was used to show the non-existence of bi-infinite geodesics [2] and local stationarity of the CGM [3]. It follows from the queuing map construction for the joint distribution (in various directions) of Busemann function from [15].

Proposition 3.8. [3, Lemma 4.5] *Let $0 < \eta < \lambda < 1$. There exists a coupling of Busemann functions B^η and B^λ such that for any fixed $x \in \mathbb{Z}^2$ and for every $k, l \in \mathbb{Z}_{>0}$, the following sets of random variables (on the horizontal line through x) are independent:*

$$\{B_{x+ie_1, x+(i+1)e_1}^\eta\}_{-k \leq i \leq -1} \quad \text{and} \quad \{B_{x+ie_1, x+(i+1)e_1}^\lambda\}_{0 \leq i \leq l-1}.$$

4 Exit time estimates

This section proves estimates on the exit time for stationary LPP processes defined in (3.4) and (3.5). These results are applied in Section 5 to prove the main theorems stated in Section 2. The first theorem is the main intermediate result towards the lower bound of Theorem 2.3. We also introduce useful lemmas that are used again later in the proof of Theorem 4.5.

Theorem 4.1. *For each $0 < \rho < 1$ there exist finite positive constants $r_0(\rho)$, $C(\rho)$ and $N_0(\rho)$ such that for all $N \geq N_0(\rho)$ and $r_0 \leq r \leq [(1 - \rho)^2 \wedge \rho^2]N^{1/3}$,*

$$\mathbb{P}^\rho \{ \forall z \text{ outside } \llbracket 0, v_N \rrbracket \text{ we have } |\mathbf{Z}^0 \rightarrow z| \geq rN^{2/3} \} \geq e^{-Cr^3}.$$

To prove this bound we tilt the probability measure to make the event likely and pay for this with a moment bound on the Radon-Nikodym derivative. This argument was introduced in [6] in the context of ASEP, and adapted to a lower bound proof of the longitudinal fluctuation exponent in the stationary LPP in Section 5.5 of the lectures [27]. The key idea is a perturbation of the parameter ρ of the stationary LPP process to $\rho \pm rN^{-1/3}$. This allows us to control the exit point on the scale $N^{2/3}$. The general idea of utilizing perturbations of order $N^{-1/3}$ goes back to the seminal paper [9].

Lemma 4.2 below is an auxiliary estimate for the proof of Theorem 4.1. It utilizes a perturbed parameter $\lambda = \rho + rN^{-1/3}$, assumed to satisfy

$$\rho < \lambda \leq c(\rho) < 1 \tag{4.1}$$

for some constant $c(\rho) < 1$, as r and N vary. Lemma 4.2 shows that, for small enough $a > 0$ and large enough $b, r > 0$, the λ -geodesic to a target point w_N slightly perturbed from v_N exits the e_1 -axis through the interval $\llbracket arN^{2/3}e_1, brN^{2/3}e_1 \rrbracket$ with high probability. This is illustrated on the right of Figure 4.1. The constants $1 - \rho$ and $2/\rho^2$ in Lemma 4.2 come from the following observation (left diagram of Figure 4.1). Start two rays at $(0, 0)$

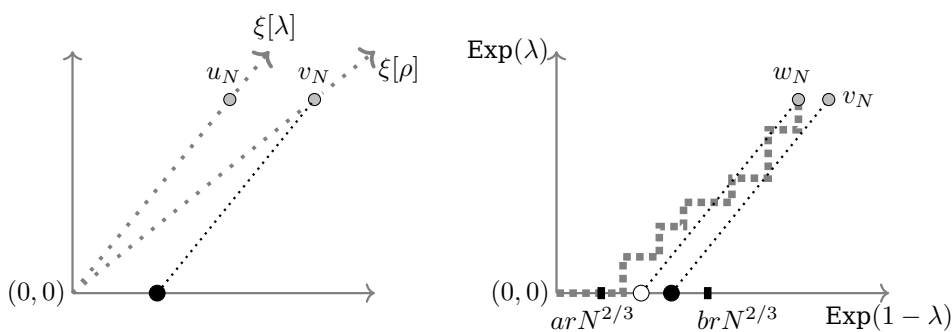


Figure 4.1: *Left:* Illustration of estimate (4.2). *Right:* Illustration of Lemma 4.2. The dotted lines have characteristic slope $\xi[\lambda]$. Consequently, with high probability, the geodesic from 0 to w_N exits through the interval $[[arN^{2/3}e_1, brN^{2/3}e_1]$.

in the directions $\xi[\rho]$ and $\xi[\lambda]$ and let u_N be the lattice point closest to the $\xi[\lambda]$ -directed ray such that $u_N \cdot e_2 = v_N \cdot e_2$. Then

$$(1 - \rho)rN^{2/3} \leq v_N \cdot e_1 - u_N \cdot e_1 \leq \frac{2}{\rho^2}rN^{2/3}. \tag{4.2}$$

Lemma 4.2. *Let $\lambda = \rho + rN^{-1/3}$ and $w_N = v_N - \lfloor \frac{1}{10}(1 - \rho)rN^{2/3} \rfloor e_1$. There exist positive constants C, N_0 that depend only on ρ such that, for any $r > 0$ and $N \geq N_0$ such that (4.1) holds, we have*

$$\mathbb{P}^\lambda \left(\frac{1}{10}(1 - \rho)rN^{2/3} \leq \mathbf{Z}^{0 \rightarrow w_N} \leq 10 \frac{2}{\rho^2}rN^{2/3} \right) \geq 1 - e^{-Cr^3}.$$

Before the proof of Lemma 4.2, we separate an observation about geodesics in the next lemma, illustrated by the left diagram of Figure 4.2. It comes from the idea of Lemma 3.2 of constructing nested LPP processes with boundary weights defined by increments of an outer LPP process. (Lemma 4.3 is proved as Lemma A.3 in the appendix of [27].)

Lemma 4.3. *Fix two base points $(0, 0)$ and $(m, -n)$ with $m, n > 0$. From these base points define coupled LPP processes $G_{(0,0),\cdot}^{(u)}$ and $G_{(m,-n),\cdot}^{(u)}$ whose boundary weights come from the increments of an LPP process $G_{u,\cdot}$ whose base point u satisfies $u \leq (0, 0)$ and $u \leq (m, -n)$. Then for $z \in ((0, 0) + \mathbb{Z}_{>0}^2) \cap ((m, -n) + \mathbb{Z}_{>0}^2)$, $\mathbf{Z}^{0 \rightarrow z} \leq m$ if and only if $\mathbf{Z}^{(m,-n) \rightarrow z} < -n$.*

Proof of Lemma 4.2. Let $a = \frac{1}{10}(1 - \rho)$, $b = 10 \frac{2}{\rho^2}$.

It suffices to show that if $r > 0$ and $N \geq N_0$ are such that (4.1) holds, then

$$\mathbb{P}^\lambda(\mathbf{Z}^{0 \rightarrow w_N} < arN^{2/3}) \leq e^{-Cr^3}, \tag{4.3}$$

$$\mathbb{P}^\lambda(\mathbf{Z}^{0 \rightarrow w_N} > brN^{2/3}) \leq e^{-Cr^3}. \tag{4.4}$$

By (4.2) the distance between the origin and the black dot on the x -axis on the right of Figure 4.1 is bounded above by $\frac{2}{\rho^2}rN^{2/3} = \frac{1}{10}brN^{2/3}$. So the distance between the black dot and $brN^{2/3}e_1$ is at least $brN^{2/3} - \frac{1}{10}brN^{2/3} = \frac{9}{10}brN^{2/3}$. Apply Lemma 3.4 to switch from the geodesic based at the origin to one based at the black dot, and apply

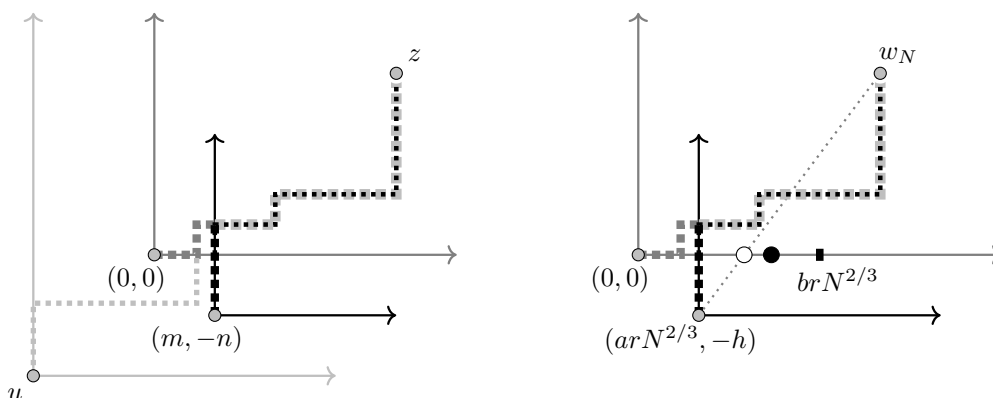


Figure 4.2: *Left:* An illustration of Lemma 4.3. As shown in the picture $\mathbf{Z}^{(0,0) \rightarrow z} \leq m$ if and only if $\mathbf{Z}^{(m,-n) \rightarrow z} < -n$. *Right:* Applying Lemma 4.3 in the proof of Lemma 4.2 to assert that $\mathbb{P}^\lambda(\mathbf{Z}^{0 \rightarrow w_N} \leq \lfloor arN^{2/3} \rfloor) = \mathbb{P}^\lambda(\mathbf{Z}^{\lfloor arN^{2/3} \rfloor, -h} \rightarrow w_N < -h)$.

Theorem 3.5 to the LPP process $G_{\text{blackdot}, \bullet}^{(0), \rho}$:

$$\begin{aligned} \mathbb{P}^\lambda(\mathbf{Z}^{0 \rightarrow w_N} > brN^{2/3}) &\leq \mathbb{P}^\lambda(\mathbf{Z}^{0 \rightarrow v_N} > brN^{2/3}) \\ &\leq \mathbb{P}^\lambda(\mathbf{Z}^{\text{black dot} \rightarrow v_N} \geq \frac{9}{10}brN^{2/3}) \leq e^{-Cr^3}. \end{aligned}$$

To prove (4.3) choose h so that $(\lfloor arN^{2/3} \rfloor, -h)$ is the closest integer point to the $(-\xi[\lambda])$ -directed ray starting at w_N (see Figure 4.2). Lemma 4.3 gives

$$\mathbb{P}^\lambda(\mathbf{Z}^{0 \rightarrow w_N} \leq \lfloor arN^{2/3} \rfloor) = \mathbb{P}^\lambda(\mathbf{Z}^{\lfloor arN^{2/3} \rfloor, -h} \rightarrow w_N < -h).$$

Theorem 3.5 states that it is unlikely for the λ -geodesic from $(\lfloor arN^{2/3} \rfloor, -h)$ to w_N to exit late in the scale $N^{2/3}$ from the y -axis, because the direction is the characteristic one $\xi[\lambda]$. Thus it suffices to show h is bounded below by some $k(\rho)rN^{2/3}$.

Using the lower bound from (4.2), the distance between the black dot and $(0, 0)$ is bounded below by $(1 - \rho)rN^{2/3} = 10arN^{2/3}$. The distance between the black dot and $\lfloor arN^{2/3} \rfloor e_1$ is bounded below by $9arN^{2/3}$, and the distance between the white dot and $\lfloor arN^{2/3} \rfloor e_1$ is bounded below by $8arN^{2/3}$. The slope of the line going through w_N and white dot is $\frac{\lambda^2}{(1-\lambda)^2}$. Thus, we have

$$h \geq \frac{\lambda^2}{(1-\lambda)^2} 8arN^{2/3}.$$

Since λ is bounded above and below by constants that depend on ρ , we get

$$h \geq k(\rho)rN^{2/3}$$

which finishes the proof. □

Proof of Theorem 4.1. For two fixed constants $0 < a < b$, we increase the weights on the intervals $[\lfloor arN^{2/3} \rfloor e_1, \lfloor brN^{2/3} \rfloor e_1]$ and $[\lfloor arN^{2/3} \rfloor e_2, \lfloor brN^{2/3} \rfloor e_2]$. The new weights are chosen so that their characteristic directions obey the left diagram of Figure 4.3 for large $N \geq N_0(\rho)$.

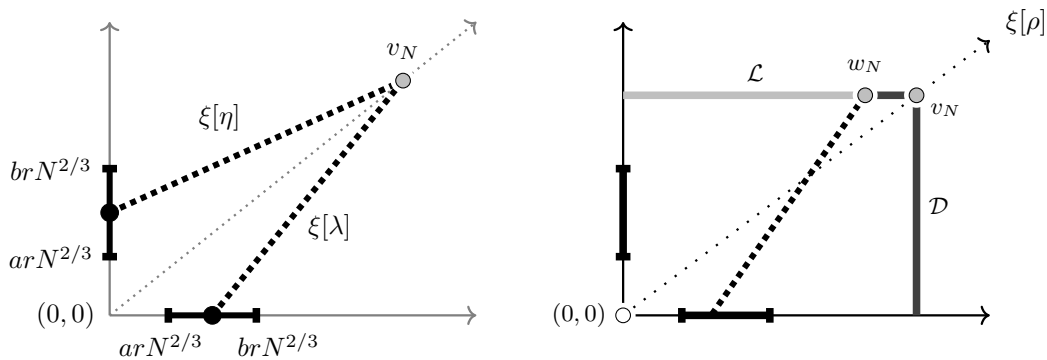


Figure 4.3: *Left*: Two dotted lines have slopes $\xi[\lambda]$ and $\xi[\eta]$. *right*: Decomposition of the north and east boundaries of $\llbracket 0, v_N \rrbracket$ into regions \mathcal{L} (light gray) and \mathcal{D} (dark gray). A small perturbation of v_N to w_N keeps the endpoint of the $-\xi[\lambda]$ ray from w_N in the interval $[arN^{2/3}, brN^{2/3}]$.

On the e_1 -axis, define

$$\lambda = \rho + \frac{r}{N^{1/3}}.$$

The assumption $0 < r \leq [(1 - \rho)^2 \wedge \rho^2]N^{1/3}$ guarantees that $0 < \lambda \leq \rho + (1 - \rho)^2 < 1$. Use $\text{Exp}(1 - \lambda)$ as the heavier weights and pick

$$a = \frac{1}{10}(1 - \rho), \quad b = 10\frac{2}{\rho^2}$$

as in Lemma 4.2.

On the e_2 -axis, we define

$$\eta = \rho - \frac{r}{N^{1/3}},$$

and the heavier weights are $\text{Exp}(\eta)$. The condition $0 < r \leq [(1 - \rho)^2 \wedge \rho^2]N^{1/3}$ guarantees that $0 < \rho - (1 - \rho)^2 \wedge \rho^2 \leq \eta < \rho$. Note that Lemma 4.2 continues to hold if a is decreased and b is increased. The constants a, b, N_0 can always be adjusted so that the situation in the left diagram of Figure 4.3 appears.

Recall the old environment of the stationary ρ -LPP process:

$$\begin{aligned} \omega_z &\sim \text{Exp}(1) && \text{for } z \in \mathbb{Z}_{>0}^2 \\ \omega_{ke_1} &\sim \text{Exp}(1 - \rho) && \text{for } k \geq 1 \\ \omega_{le_2} &\sim \text{Exp}(\rho) && \text{for } l \geq 1. \end{aligned}$$

The new environment $\tilde{\omega}$ increases the weights in the two intervals on the axes:

$$\begin{aligned} \tilde{\omega}_z &= \omega_z && \text{for } z \notin \llbracket [arN^{2/3}]e_1, [brN^{2/3}]e_1 \rrbracket \cup \llbracket [arN^{2/3}]e_2, [brN^{2/3}]e_2 \rrbracket \\ \tilde{\omega}_{ke_1} &= \frac{1 - \rho}{1 - \lambda} \omega_{ke_1} && \text{for } ke_1 \in \llbracket [arN^{2/3}]e_1, [brN^{2/3}]e_1 \rrbracket \\ \tilde{\omega}_{le_2} &= \frac{\rho}{\eta} \omega_{le_2} && \text{for } le_2 \in \llbracket [arN^{2/3}]e_2, [brN^{2/3}]e_2 \rrbracket. \end{aligned}$$

Denote the probability measure for the environment $\tilde{\omega}$ by $\tilde{\mathbb{P}}$. The goal is the estimate

$$\tilde{\mathbb{P}}(A) \equiv \tilde{\mathbb{P}}\{\forall z \text{ outside } \llbracket 0, v_N \rrbracket \text{ we have } |\mathbf{Z}^{0 \rightarrow z}| \geq arN^{2/3}\} \geq 1/2 \quad (4.5)$$

where A denotes the event in braces. We check that this implies Theorem 4.1. The Cauchy-Schwartz inequality gives

$$1/2 \leq \tilde{\mathbb{P}}(A) = \mathbb{E}^\rho[\mathbf{1}_A f_N] \leq (\mathbb{P}^\rho(A))^{1/2} (\mathbb{E}^\rho[f^2])^{1/2} \tag{4.6}$$

where f is the Radon-Nikodym derivative. Lemma A.2 gives the bound

$$\mathbb{E}^\rho[f^2] \leq e^{Cr^3} \tag{4.7}$$

and then (4.6) and (4.7) imply the lower bound

$$\mathbb{P}^\rho(A) \geq \frac{1}{2} e^{-Cr^3}.$$

Note that the event A in (4.5) has the lower bound $\geq arN^{2/3}$. To replace this with $\geq rN^{2/3}$, as required for Theorem 4.1, modify the constant C .

To show (4.5) we bound its complement:

$$\tilde{\mathbb{P}}\{\exists z \text{ outside } \llbracket 0, v_N \rrbracket \text{ such that } |\mathbf{Z}^{0 \rightarrow z}| \leq arN^{2/3}\} \leq e^{-Cr^3}. \tag{4.8}$$

We treat the case $1 \leq \mathbf{Z}^{0 \rightarrow z} \leq arN^{2/3}$ of (4.8). The same arguments give the analogous bound for the case $-arN^{2/3} \leq \mathbf{Z} \leq -1$. Define $w_N = v_N - \lfloor \frac{1}{10}(1-\rho)rN^{2/3} \rfloor e_1$, and break up the northeast boundary of $\llbracket 0, v_N \rrbracket$ into two regions \mathcal{L} and \mathcal{D} as in the diagram on the right of Figure 4.3.

First consider geodesics that hit \mathcal{D} . Let $\sigma_1^{0 \rightarrow x}$ denote the exit time of the optimal $0 \rightarrow x$ path among those paths whose first step is e_1 .

$$\begin{aligned} \tilde{\mathbb{P}}\{\exists z \in \mathcal{D} : 1 \leq \mathbf{Z}^{0 \rightarrow z} < arN^{2/3}\} &\leq \tilde{\mathbb{P}}\{\exists z \in \mathcal{D} : \sigma_1^{0 \rightarrow z} < arN^{2/3}\} \\ &\leq \tilde{\mathbb{P}}\{\sigma_1^{0 \rightarrow w_N} < arN^{2/3}\} \leq \tilde{\mathbb{P}}\{\sigma_1^{0 \rightarrow w_N} \notin \llbracket \lfloor arN^{2/3} \rfloor e_1, \lfloor brN^{2/3} \rfloor e_1 \rrbracket\} \\ &\leq \mathbb{P}^\lambda\{\sigma_1^{0 \rightarrow w_N} \notin \llbracket \lfloor arN^{2/3} \rfloor e_1, \lfloor brN^{2/3} \rfloor e_1 \rrbracket\} \\ &\leq \mathbb{P}^\lambda\{\mathbf{Z}^{0 \rightarrow w_N} \notin \llbracket \lfloor arN^{2/3} \rfloor e_1, \lfloor brN^{2/3} \rfloor e_1 \rrbracket\} \leq e^{-Cr^3}. \end{aligned} \tag{4.9}$$

The second inequality comes from the uniqueness of maximizing paths: the maximizing path to w_N cannot go to the right of a maximizing path to \mathcal{D} . The switch from $\tilde{\mathbb{P}}$ to \mathbb{P}^λ increases the boundary weights on the e_1 axis outside the interval $\llbracket \lfloor arN^{2/3} \rfloor e_1, \lfloor brN^{2/3} \rfloor e_1 \rrbracket$, hence the fourth inequality. The last inequality is from Lemma 4.2.

Consider the light gray region \mathcal{L} . The switch from $\tilde{\mathbb{P}}$ to \mathbb{P}^ρ decreases certain boundary weights outside the range $\llbracket e_1, \lceil arN^{2/3} - 1 \rceil e_1 \rrbracket$ and gives the first inequality below.

$$\begin{aligned} \tilde{\mathbb{P}}\{\exists z \in \mathcal{L} : 1 \leq \mathbf{Z}^{0 \rightarrow z} < arN^{2/3}\} &\leq \mathbb{P}^\rho\{\exists z \in \mathcal{L} : 1 \leq \mathbf{Z}^{0 \rightarrow z} < arN^{2/3}\} \\ &\leq \mathbb{P}^\rho\{\exists z \in \mathcal{L} : \mathbf{Z}^{0 \rightarrow z} \geq 1\} \leq \mathbb{P}^\rho\{\mathbf{Z}^{0 \rightarrow w_N} \geq 1\} \leq e^{-Cr^3}. \end{aligned} \tag{4.10}$$

The last inequality follows from bound (3.8) in Corollary 3.6.

Combining (4.9) and (4.10) gives

$$\tilde{\mathbb{P}}\{\exists z \text{ outside } \llbracket 0, v_N \rrbracket \text{ such that } 1 \leq \mathbf{Z}^{0 \rightarrow z} \leq arN^{2/3}\} \leq e^{-Cr^3}.$$

The proof is complete. □

The next theorem is the main intermediate result towards the lower bound of Theorem 2.2.

Theorem 4.4. *For each $0 < \rho < 1$ there exist finite positive constants $\delta_0(\rho)$, $C(\rho)$ and $N_0(\rho)$ such that for all $N \geq N_0(\rho)$ and $N^{-2/3} \leq \delta \leq \delta_0(\rho)$,*

$$\mathbb{P}^\rho\{\exists z \text{ outside } \llbracket 0, v_N \rrbracket \text{ such that } |\mathbf{Z}^{0 \rightarrow z}| \leq \delta N^{2/3}\} \geq C(\rho)\delta.$$

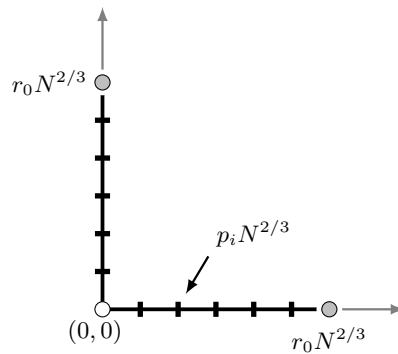


Figure 4.4: Partition of the range of $\mathbf{Z}^{0 \rightarrow v_N}$ in the event in (4.11). The origin is not necessarily a partition point.

Proof. Utilizing Theorem 3.5, fix constants r_0 , C_0 and N_0 (depending on ρ) such that, for $N \geq N_0$,

$$\mathbb{P}^\rho \{ |\mathbf{Z}^{0 \rightarrow v_N + e_1 + e_2}| \leq r_0 N^{2/3} \} \geq 1/2. \tag{4.11}$$

Set $v'_N = v_N + e_1 + e_2$. Given small $\delta > N^{-2/3}$, partition $[-r_0, r_0]$ as

$$-r_0 = p_0 < p_1 < \dots < p_{\lfloor \frac{2r_0}{\delta} \rfloor} < p_{\lfloor \frac{2r_0}{\delta} \rfloor + 1} = r_0$$

with mesh $p_{i+1} - p_i \leq \delta$. See Figure 4.4. By (4.11) there exists an integer $i^* \in [0, \lfloor \frac{2r_0}{\delta} \rfloor]$ such that

$$\mathbb{P}^\rho \{ p_{i^*} N^{2/3} \leq \mathbf{Z}^{0 \rightarrow v'_N} \leq p_{i^*+1} N^{2/3} \} \geq \frac{\frac{1}{2}\delta}{2r_0} = C(\rho)\delta. \tag{4.12}$$

We cannot control the exact location of i^* . We compensate by varying the endpoint around v'_N . Let

$$A_N = \llbracket v'_N - r_0 N^{2/3} e_1, v'_N \rrbracket \cup \llbracket v'_N - r_0 N^{2/3} e_2, v'_N \rrbracket$$

denote the set of lattice points on the boundary of the rectangle $\llbracket 0, v'_N \rrbracket$ within distance $r_0 N^{2/3}$ of the upper right corner v'_N . We claim that for any integer $i \in [0, \lfloor \frac{2r_0}{\delta} \rfloor]$,

$$\mathbb{P}^\rho \{ \exists z \in A_N : |\mathbf{Z}^{0 \rightarrow z}| \leq \delta N^{2/3} \} \geq \mathbb{P}^\rho \{ p_i N^{2/3} \leq \mathbf{Z}^{0 \rightarrow v'_N} \leq p_{i+1} N^{2/3} \}. \tag{4.13}$$

Then bounds (4.12) and (4.13) imply

$$\mathbb{P}^\rho \{ \exists z \in A_N : |\mathbf{Z}^{0 \rightarrow z}| \leq \delta N^{2/3} \} \geq C(\rho)\delta, \tag{4.14}$$

and Theorem 4.4 directly follows from (4.14).

We prove claim (4.13). If $p_i \leq 0 \leq p_{i+1}$, (4.13) is immediate. We argue the case $p_{i+1} > p_i > 0$, the other one being analogous. Set $z = (\lfloor p_i N^{2/3} \rfloor - 1)e_1$ and apply Lemma 3.4 to the LPP process $G_{z, \cdot}^{(0), \rho}$. Then

$$\begin{aligned} \mathbb{P}^\rho \{ p_i N^{2/3} \leq \mathbf{Z}^{0 \rightarrow v'_N} \leq p_{i+1} N^{2/3} \} &\leq \mathbb{P}^\rho \{ 1 \leq \mathbf{Z}^{0 \rightarrow v'_N - (\lfloor p_i N^{2/3} \rfloor - 1)e_1} \leq \delta N^{2/3} \} \\ &\leq \mathbb{P}^\rho \{ \exists z \in A_N : |\mathbf{Z}^{0 \rightarrow z}| \leq \delta N^{2/3} \}. \quad \square \end{aligned}$$

The remainder of this section proves the main intermediate result towards the upper bound of Theorem 2.2. It quantifies the lower bound on the exit point on the scale $N^{2/3}$. This strengthens the estimates accessible without integrable probability, for previously no quantification was attained (Theorem 2.2(b) in [4]). The proof is based on the ideas from the recent work of [2, 3].

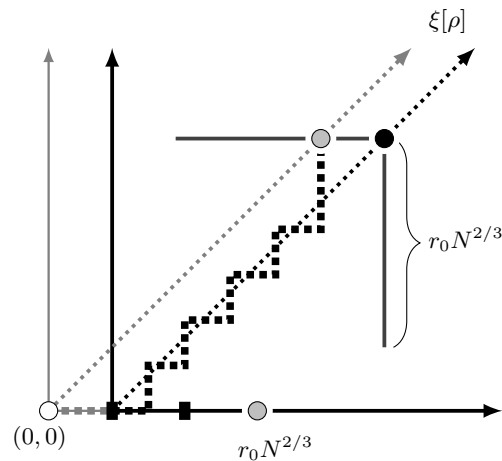


Figure 4.5: The setup for proving (4.13).

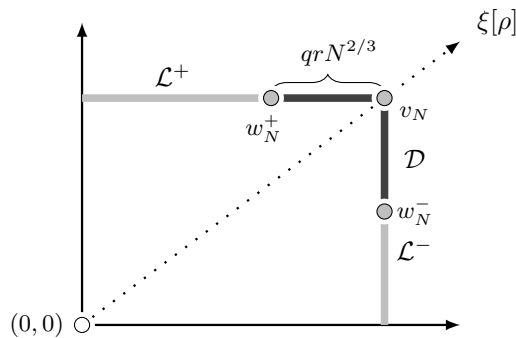


Figure 4.6: The north and east boundaries of $\llbracket 0, v_N \rrbracket$ are decomposed into \mathcal{L}^\pm (light gray) and \mathcal{D} (dark gray). The parameter q is less than some small constant that depends only on ρ .

Theorem 4.5. For each $0 < \rho < 1$ there exist finite positive constants $\delta_0(\rho)$, $C(\rho)$ and $N_0(\rho)$ such that for all $0 < \delta \leq \delta_0(\rho)$ and $N \geq N_0(\rho)$,

$$\mathbb{P}^\rho \left\{ \exists z \text{ outside } \llbracket 0, v_N \rrbracket \text{ such that } |\mathbf{Z}^{0 \rightarrow z}| \leq \delta N^{2/3} \right\} \leq C |\log \delta|^{2/3} \delta.$$

Proof. We prove the case $1 \leq \mathbf{Z} \leq \delta N^{2/3}$. The proof for $-\delta N^{2/3} \leq \mathbf{Z} \leq -1$ is similar. It suffices to look at the north and east boundaries of $\llbracket 0, v_N \rrbracket$ since any geodesic from 0 to outside of $\llbracket 0, v_N \rrbracket$ crosses the boundary. Decompose these boundaries into three parts \mathcal{D} and \mathcal{L}^\pm as in Figure 4.6, with

$$w_N^+ = v_N - \lfloor qr N^{2/3} \rfloor e_1 \quad \text{and} \quad w_N^- = v_N - \lfloor qr N^{2/3} \rfloor e_2$$

where q is a small positive constant chosen later, and $r = (|\log \delta|/C)^{1/3}$ where C is the constant in the right-hand side of the estimate in Theorem 3.5. The dark gray set \mathcal{D} comprises the vertices between w_N^+ and w_N^- in the north-east corner of the boundary of the rectangle $\llbracket 0, v_N \rrbracket$.

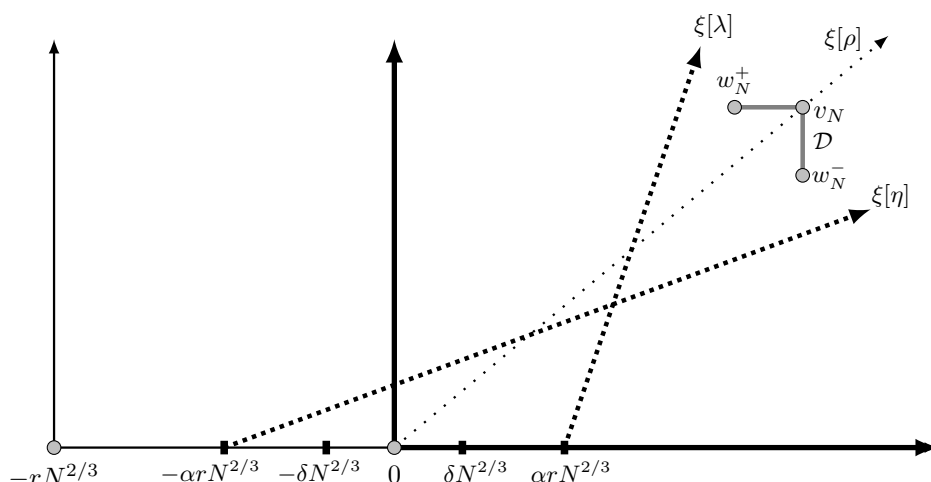


Figure 4.7: Illustration of the set \mathcal{D} , the nested LPP processes, and three characteristic directions. The parameters $q = \alpha$ are less than some small constant that depends only on ρ , δ is a small positive constant in $(0, \delta_0)$, and r is a large constant with $r = (|\log \delta|/C)^{1/3}$.

Consider first, the dark gray portion \mathcal{D} . Take $0 < \delta \leq \delta_0 = \frac{9}{10}$, where the bound $\frac{9}{10}$ may be decreased later in the proof. Our goal is to estimate

$$\mathbb{P}^\rho \{ \exists z \in \mathcal{D} \text{ such that } 1 \leq \mathbf{Z}^{0 \rightarrow z} \leq \delta N^{2/3} \}. \tag{4.15}$$

To do this, we place the stationary LPP process on $0 + \mathbb{Z}_{\geq 0}^2$ as a nested LPP process inside a larger stationary LPP process on the quadrant $-[rN^{2/3}]e_1 + \mathbb{Z}_{\geq 0}^2$, as shown in Figure 4.7. From the relation between geodesics of two nested LPP processes given in Lemma 3.4,

$$\begin{aligned} & \mathbb{P}^\rho \{ \exists z \in \mathcal{D} : 1 \leq \mathbf{Z}^{0 \rightarrow z} \leq \delta N^{2/3} \} \\ & \leq \mathbb{P}^\rho \{ \exists z \in \mathcal{D} : [rN^{2/3}] - \delta N^{2/3} \leq \mathbf{Z}^{-[rN^{2/3}]e_1 \rightarrow z} \leq [rN^{2/3}] + \delta N^{2/3} \} \end{aligned}$$

Thus, it suffices to obtain an upper bound for the second line above. To continue, we describe the rest of the setup shown in Figure 4.7.

The probability in (4.15) vanishes if $\delta N^{2/3} < 1$ and hence we can always assume

$$N \geq \delta^{-3/2}. \tag{4.16}$$

Introduce the perturbed parameters

$$\lambda = \rho + \frac{r}{N^{1/3}} \quad \text{and} \quad \eta = \rho - \frac{r}{N^{1/3}}. \tag{4.17}$$

We require the following bounds to hold for these two parameters

$$\rho < \lambda \leq \rho + \frac{\rho \wedge (1 - \rho)}{2} < 1 \quad \text{and} \quad 0 < \rho - \frac{\rho \wedge (1 - \rho)}{2} \leq \eta < \rho. \tag{4.18}$$

The point of the choice $\rho \pm \frac{\rho \wedge (1 - \rho)}{2}$ is only to bound λ and η from above and below by two constants strictly inside $(0, 1)$ and that depend only on ρ . These two requirements can be rewritten as

$$N \geq \left(\frac{2r}{\rho \wedge (1 - \rho)} \right)^3.$$

With (4.16), this bound on N is automatically satisfied as long as $\delta^{-3/2} \geq \left(\frac{2r}{\rho \wedge (1-\rho)}\right)^3$. With $r = \left(\frac{\lfloor \log \delta \rfloor}{C}\right)^{1/3}$, we can ensure this by considering $\delta > 0$ subject to

$$\delta \leq \delta_0(\rho) = \left(\frac{1}{2}C(\rho \wedge (1-\rho))\right)^3 \wedge \frac{9}{10}. \tag{4.19}$$

Our next step is to fix q and α small enough so that the $\xi[\eta]$ - and $\xi[\lambda]$ -directed rays started at the points $\pm \lfloor \alpha r N^{2/3} \rfloor e_1$ avoid \mathcal{D} as shown in Figure 4.7. As in Figure 4.1, let u_N be the lattice point closest to where the $\xi[\lambda]$ -ray from the origin crosses the north boundary of $\llbracket 0, v_N \rrbracket$. Then from (4.2) we have

$$v_N \cdot e_1 - u_N \cdot e_1 \geq (1-\rho)rN^{2/3}.$$

Shift the starting point of the $\xi[\lambda]$ -ray from the origin to $\lfloor \alpha r N^{2/3} \rfloor e_1$, and let u'_N be the new crossing point on the north boundary of $\llbracket 0, v_N \rrbracket$. By picking $q = \alpha = \frac{1-\rho}{10}$, the following lower bound holds:

$$w_N^+ \cdot e_1 - u'_N \cdot e_1 \geq \frac{1-\rho}{2}rN^{2/3}. \tag{4.20}$$

This gives us the desired picture for $\xi[\lambda]$ shown in Figure 4.7. The argument for the $\xi[\eta]$ -directed ray is similar. We may need to decrease α and q further to achieve this but their values depend only on ρ . At last, once α is fixed, $r = \left(\frac{\lfloor \log \delta \rfloor}{C}\right)^{1/3}$ allows us to decrease δ_0 further so that $\delta < \frac{1}{3}\alpha r$ for each $0 < \delta \leq \delta_0$. This completes the description of the setup in Figure 4.7.

Now, to bound

$$\mathbb{P}^\rho \{ \exists z \in \mathcal{D} : \lfloor rN^{2/3} \rfloor - \delta N^{2/3} \leq \mathbf{Z}^{-\lfloor rN^{2/3} \rfloor e_1} \rightarrow z \leq \lfloor rN^{2/3} \rfloor + \delta N^{2/3} \},$$

we first bound the probability

$$\mathbb{P}^\rho \{ \exists z \in \mathcal{D} : \mathbf{Z}^{-\lfloor rN^{2/3} \rfloor e_1} \rightarrow z = \lfloor rN^{2/3} \rfloor + t_0 \} \tag{4.21}$$

where t_0 is a fixed integer in $\llbracket -\lfloor \delta N^{2/3} \rfloor, \lfloor \delta N^{2/3} \rfloor \rrbracket$.

For $z \in \mathcal{D}$ and $i \in \llbracket -\lfloor \alpha r N^{2/3} \rfloor + 1, \lfloor \alpha r N^{2/3} \rfloor \rrbracket$, define horizontal increments

$$\tilde{I}_i^z = G_{(i-1,1),z} - G_{(i,1),z}$$

on the horizontal line $y = 1$. Define a 2-sided walk $\{Z_n^{z,t_0}\}_{n \in \llbracket -\lfloor \alpha r N^{2/3} \rfloor + 1, \lfloor \alpha r N^{2/3} \rfloor \rrbracket}$ by setting $Z_{t_0}^{z,t_0} = 0$ and

$$Z_n^{z,t_0} - Z_{n-1}^{z,t_0} = I_n - \tilde{I}_n^z.$$

The boundary weights I_n are those of the ρ -LPP process in the quadrant $-\lfloor rN^{2/3} \rfloor e_1 + \mathbf{Z}_{\geq 0}^2$. On the event

$$\{ \mathbf{Z}^{-\lfloor rN^{2/3} \rfloor e_1} \rightarrow z = \lfloor rN^{2/3} \rfloor + t_0 \}$$

the geodesic goes through the vertical unit edge $\llbracket (t_0, 0), (t_0, 1) \rrbracket$. This implies that the walk $\{Z_n^{z,t_0}\}_{n \in \llbracket -\lfloor \alpha r N^{2/3} \rfloor + 1, \lfloor \alpha r N^{2/3} \rfloor \rrbracket}$ attains its unique maximum at $n = t_0$. To see this, note that for $n \in \llbracket -\lfloor \alpha r N^{2/3} \rfloor + 1, \lfloor \alpha r N^{2/3} \rfloor \rrbracket \setminus \{t_0\}$, we have almost surely

$$\begin{aligned} & G_{-\lfloor rN^{2/3} \rfloor e_1, (t_0, 0)}^\rho + G_{(t_0, 1), z} > G_{-\lfloor rN^{2/3} \rfloor e_1, (n, 0)}^\rho + G_{(n, 1), z} \\ \implies & G_{-\lfloor rN^{2/3} \rfloor e_1, (t_0, 0)}^\rho - G_{-\lfloor rN^{2/3} \rfloor e_1, (n, 0)}^\rho > G_{(n, 1), z} - G_{(t_0, 1), z}. \end{aligned} \tag{4.22}$$

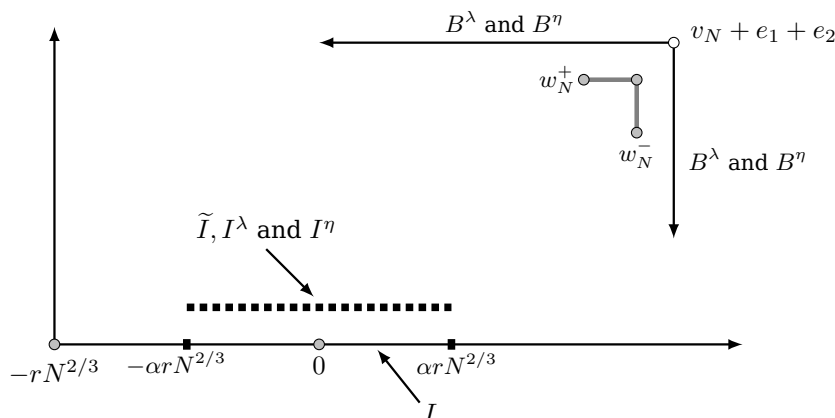


Figure 4.8: Setup for the stationary LPP processes with Busemann increments.

From this,

- for $n > t_0$, (4.22) $\implies -\sum_{i=t_0+1}^n I_i > -\sum_{i=t_0+1}^n \tilde{I}_i^z \implies 0 > Z_n^{z,t_0} - Z_{t_0}^{z,t_0}$;
- for $n < t_0$, (4.22) $\implies \sum_{i=n+1}^{t_0} I_i > \sum_{i=n+1}^{t_0} \tilde{I}_i^z \implies Z_{t_0}^{z,t_0} - Z_n^{z,t_0} > 0$.

Since $\delta \leq \frac{1}{3}\alpha r$, $t_0 \in [-\frac{1}{3}\alpha rN^{2/3}, \frac{1}{3}\alpha rN^{2/3}]$. Also because the value of the walk at t_0 is zero, we now have

$$\begin{aligned}
 (4.21) &\leq \mathbb{P}\left\{\exists z \in \mathcal{D} : \operatorname{argmax}_{n \in [-\lfloor \alpha rN^{2/3} \rfloor + 1, \lfloor \alpha rN^{2/3} \rfloor]} \{Z_n^{z,t_0}\} = t_0\right\} \\
 &\leq \mathbb{P}\left(\left\{\exists z \in \mathcal{D} : Z_n^{z,t_0} < 0 \text{ for } n \in (t_0, t_0 + \lfloor \frac{1}{2}\alpha rN^{2/3} \rfloor]\right\} \right. \\
 &\quad \left. \cap \left\{\exists z \in \mathcal{D} : Z_n^{z,t_0} < 0 \text{ for } n \in [t_0 - \lfloor \frac{1}{2}\alpha rN^{2/3} \rfloor, t_0)\right\}\right)
 \end{aligned}
 \tag{4.23}$$

Due to the relative positions of w_N^\pm and z , Lemma 3.1 implies that

$$\tilde{I}_i^{w_N^-} \leq \tilde{I}_i^z \leq \tilde{I}_i^{w_N^+} \quad \forall i \in [-\lfloor \alpha rN^{2/3} \rfloor + 1, \lfloor \alpha rN^{2/3} \rfloor] \text{ and } z \in \mathcal{D}.
 \tag{4.24}$$

Hence for any $z \in \mathcal{D}$,

$$Z_n^{z,t_0} \geq Z_n^{w_N^+,t_0} \quad \text{for } n > t_0 \quad \text{and} \quad Z_n^{z,t_0} \geq Z_n^{w_N^-,t_0} \quad \text{for } n < t_0.$$

Therefore, we may bound (4.23) by

$$\begin{aligned}
 (4.23) &\leq \mathbb{P}\left(\left\{Z_n^{w_N^+,t_0} < 0 \text{ for } n \in (t_0, t_0 + \lfloor \frac{1}{2}\alpha rN^{2/3} \rfloor]\right\} \right. \\
 &\quad \left. \cap \left\{Z_n^{w_N^-,t_0} < 0 \text{ for } n \in [t_0 - \lfloor \frac{1}{2}\alpha rN^{2/3} \rfloor, t_0)\right\}\right).
 \end{aligned}
 \tag{4.25}$$

We bring the Busemann increments defined by the bulk weights $\{\omega_x\}_{x \in [-\lfloor rN^{2/3} \rfloor e_1 + \mathbb{Z}_{>0}^2, \lfloor rN^{2/3} \rfloor e_1 + v_N + e_1 + e_2]}$ into the picture. To each edge on the the north and east sides of the rectangle $[-\lfloor rN^{2/3} \rfloor e_1, v_N + e_1 + e_2]$, we attach λ - and η -directed Busemann increments, coupled as in Proposition 3.8. This is depicted in Figure 4.8. Together with the bulk weights in $[-\lfloor rN^{2/3} \rfloor e_1 + e_2, v_N]$, these define stationary LPP processes with north and east

boundaries, denoted by $G_{x,v_N+e_1+e_2}^{\lambda,NE}$ and $G_{x,v_N+e_1+e_2}^{\eta,NE}$ for $x \in \llbracket(-\lfloor rN^{2/3} \rfloor, 1), v_N \rrbracket$. This is the construction explained after Theorem 3.7.

On the horizontal line $y = 1$ we have for $i \in \llbracket -\lfloor \alpha r N^{2/3} \rfloor + 1, \lfloor \alpha r N^{2/3} \rfloor \rrbracket$ the increments

$$\begin{aligned} I_i^\lambda &= G_{(i-1,1),v_N+e_1+e_2}^{\lambda,NE} - G_{(i,1),v_N+e_1+e_2}^{\lambda,NE} = B_{(i-1,1),(i,1)}^\lambda \\ \text{and } I_i^\eta &= G_{(i-1,1),v_N+e_1+e_2}^{\eta,NE} - G_{(i,1),v_N+e_1+e_2}^{\eta,NE} = B_{(i-1,1),(i,1)}^\eta \end{aligned} \tag{4.26}$$

where the latter equalities are instances of (3.12).

Lemma 4.6. *The event*

$$A = \{ \forall i \in \llbracket -\lfloor \alpha r N^{2/3} \rfloor + 1, \lfloor \alpha r N^{2/3} \rfloor \rrbracket : I_i^\eta \leq \tilde{I}_i^{w_N^-} \leq \tilde{I}_i^{w_N^+} \leq I_i^\lambda \} \tag{4.27}$$

satisfies $\mathbb{P}(A^c) \leq e^{-Cr^3}$.

Proof. The middle inequality is already in (4.24). We give the proof for

$$\mathbb{P}\{ \forall i \in \llbracket -\lfloor \alpha r N^{2/3} \rfloor + 1, \lfloor \alpha r N^{2/3} \rfloor \rrbracket : \tilde{I}_i^{w_N^+} \leq I_i^\lambda \} \geq 1 - e^{-Cr^3}.$$

The similar argument for the remaining part is omitted.

We argue first that $\tilde{I}_i^{w_N^+} \leq I_i^\lambda$ is implied for the entire range of indices i when the geodesic of $G_{(\lfloor \alpha r N^{2/3} \rfloor, 1), v_N+e_1+e_2}^{\lambda,NE}$ exits the north boundary to the left of the point $w_N^+ + e_2$.

For $x \in \llbracket(-\lfloor rN^{2/3} \rfloor, 1), w_N^+ + e_2 \rrbracket$, let $G_{x,w_N^+ + e_2}^{\lambda,N}$ denote the last-passage time from x to $w_N^+ + e_2$ that uses the B^λ increment weights on the north boundary (superscript N for north).

The exit time $\mathbf{Z}^{\lambda,NE, x \rightarrow v_N+e_1+e_2}$ records the signed distance from the vertex $v_N + e_1 + e_2$ to the point where the geodesic of $G_{x,v_N+e_1+e_2}^{\lambda,NE}$ enters the north (as a positive value) or the east (as a negative value) boundary of the rectangle $\llbracket x, v_N + e_1 + e_2 \rrbracket$. Since geodesics cannot cross, the event

$$\left\{ \mathbf{Z}^{\lambda,NE, (\lfloor \alpha r N^{2/3} \rfloor, 1) \rightarrow v_N+e_1+e_2} > qrN^{2/3} \right\}$$

implies

$$\bigcap_{i \in \llbracket -\lfloor \alpha r N^{2/3} \rfloor + 1, \lfloor \alpha r N^{2/3} \rfloor \rrbracket} \left\{ \mathbf{Z}^{\lambda,NE, (i,1) \rightarrow v_N+e_1+e_2} > qrN^{2/3} \right\}.$$

This further implies

$$\begin{aligned} G_{(i-1,1),w_N^+ + e_2}^{\lambda,N} - G_{(i,1),w_N^+ + e_2}^{\lambda,N} &= G_{(i-1,1),v_N+e_1+e_2}^{\lambda,NE} - G_{(i,1),v_N+e_1+e_2}^{\lambda,NE} \\ \forall i \in \llbracket -\lfloor \alpha r N^{2/3} \rfloor + 1, \lfloor \alpha r N^{2/3} \rfloor \rrbracket. \end{aligned} \tag{4.28}$$

In the derivation below, Lemma 3.1 gives the first inequality. The equality in the second line is (4.28) which is valid on the event $\left\{ \mathbf{Z}^{\lambda,NE, (\lfloor \alpha r N^{2/3} \rfloor, 1) \rightarrow v_N+e_1+e_2} > qrN^{2/3} \right\}$:

$$\begin{aligned} \tilde{I}_i^{w_N^+} &= G_{(i-1,1),w_N^+} - G_{(i,1),w_N^+} \leq G_{(i-1,1),w_N^+ + e_2}^{\lambda,N} - G_{(i,1),w_N^+ + e_2}^{\lambda,N} \\ &= G_{(i-1,1),v_N+e_1+e_2}^{\lambda,NE} - G_{(i,1),v_N+e_1+e_2}^{\lambda,NE} = I_i^\lambda \\ &\forall i \in \llbracket -\lfloor \alpha r N^{2/3} \rfloor + 1, \lfloor \alpha r N^{2/3} \rfloor \rrbracket. \end{aligned}$$

This finishes the proof that $\mathbf{Z}^{\lambda,NE, (\lfloor \alpha r N^{2/3} \rfloor, 1) \rightarrow v_N+e_1+e_2} > qrN^{2/3}$ implies $\tilde{I}_i^{w_N^+} \leq I_i^\lambda$ for all $i \in \llbracket -\lfloor \alpha r N^{2/3} \rfloor + 1, \lfloor \alpha r N^{2/3} \rfloor \rrbracket$.

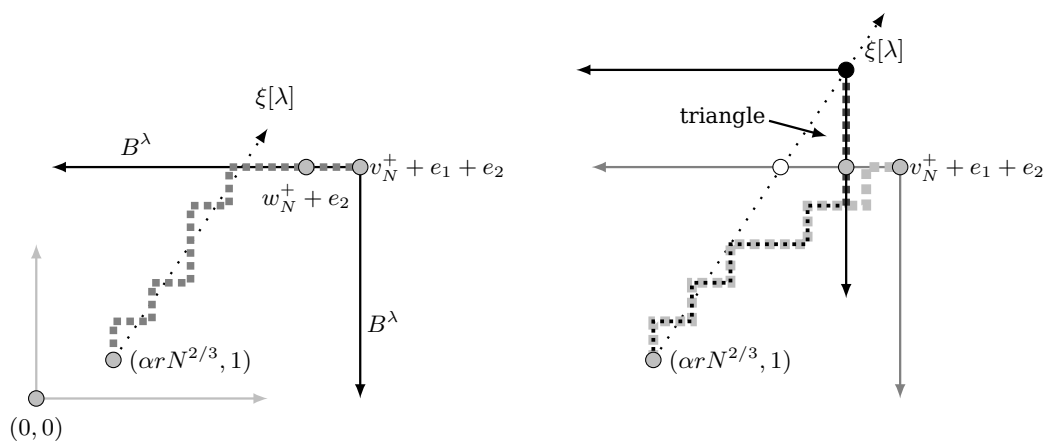


Figure 4.9: *Left*: The likely behavior of the geodesic of $G_{([\alpha r N^{2/3}], 1), v_N^+ + e_1 + e_2}^{\lambda, NE}$. It enters the north boundary to the left of $w_N^+ + e_2$. *Right*: The unlikely behavior of the geodesic of $G_{([\alpha r N^{2/3}], 1), v_N^+ + e_1 + e_2}^{\lambda, NE}$. In this case, the dark dotted line is the geodesic between the black dot and $([\alpha r N^{2/3}], 1)$. It spends an atypically large amount of time on the boundary.

Finally, we show that

$$\mathbb{P} \left\{ Z^{\lambda, NE}, ([\alpha r N^{2/3}], 1) \rightarrow v_N^+ + e_1 + e_2 > q r N^{2/3} \right\} \geq 1 - e^{-C r^3}.$$

This follows from the standard exit time estimate. As shown in the left diagram of Figure 4.9, the geodesic of $G_{([\alpha r N^{2/3}], 1), v_N^+ + e_1 + e_2}^{\lambda, NE}$ (gray dotted line) tends to follow the characteristic direction $\xi[\lambda]$ which means it enters the north boundary on the left of $w_N^+ + e_2$. Else, by Lemma 4.3, there exists a parameter- λ stationary LPP process whose geodesic (black dotted line in the right diagram of Figure 4.9) in the characteristic direction spends excessive time on the boundary. The precise argument goes as follows.

Consider the right triangle whose vertices are the black, gray and white dots highlighted in the right diagram of Figure 4.9. The distance between the white and gray dots is bounded below by $\frac{1-\rho}{2} r N^{2/3}$ by (4.20). Then, the distance between the black dot and the gray dot is at least $\frac{\lambda^2}{(1-\lambda)^2} \frac{1-\rho}{2} r N^{2/3}$ where $\frac{\lambda^2}{(1-\lambda)^2}$ is the slope of the hypotenuse. By Theorem 3.5, the probability that the geodesic shown as the black dotted line remains on the boundary throughout the segment between the black and the gray dot is bounded above by $e^{-C r^3}$. Here C depends on λ , and bounds (4.18) turn this into a dependence on ρ . This completes the proof of Lemma 4.6. \square

With these new horizontal increments I^λ and I^η , define two more 2-sided random walks Z_n^{λ, t_0} and Z_n^{η, t_0} with $Z_{t_0}^{\lambda, t_0} = Z_{t_0}^{\eta, t_0} = 0$ and

$$\begin{aligned} Z_n^{\lambda, t_0} - Z_{n-1}^{\lambda, t_0} &= I_n - I_n^\lambda, \\ Z_n^{\eta, t_0} - Z_{n-1}^{\eta, t_0} &= I_n - I_n^\eta, \end{aligned}$$

On the event A from (4.27),

$$Z_n^{\lambda, t_0} \leq Z_n^{w_N^+, t_0} \text{ for } n > t_0 \quad \text{and} \quad Z_n^{\eta, t_0} \leq Z_n^{w_N^-, t_0} \text{ for } n < t_0.$$

We continue our bound

$$\mathbb{P}(\text{event in (4.25)} \cap A) \leq \mathbb{P}\left(\left\{Z_n^{\lambda,t_0} < 0 \text{ for } n \in (t_0, t_0 + \lfloor \frac{1}{2}\alpha r N^{2/3} \rfloor]\right\} \cap \left\{Z_n^{\eta,t_0} < 0 \text{ for } n \in [t_0 - \lfloor \frac{1}{2}\alpha r N^{2/3} \rfloor, t_0)\right\}\right). \tag{4.29}$$

From Proposition 3.8, the increment variables $\{I_{(i,1)}^\lambda\}_{i>t_0} \cup \{I_{(i,1)}^\eta\}_{i\leq t_0}$ are independent, and these are independent of the boundary weights $\{I_i\}$ by construction. Thus, the two events on the right-hand side above are independent. This gives

$$(4.29) = \mathbb{P}\left\{Z_n^{\lambda,t_0} < 0 \text{ for } n \in (t_0, t_0 + \lfloor \frac{1}{2}\alpha r N^{2/3} \rfloor]\right\} \cdot \mathbb{P}\left\{Z_n^{\eta,t_0} < 0 \text{ for } n \in [t_0 - \lfloor \frac{1}{2}\alpha r N^{2/3} \rfloor, t_0)\right\}.$$

The steps of the random walks in the two probabilities above have distributions $\text{Exp}(1 - \rho) - \text{Exp}(1 - \lambda)$ and $\text{Exp}(1 - \eta) - \text{Exp}(1 - \rho)$, respectively. By Lemma A.1 each of the probabilities is bounded above by $C(\rho)rN^{-1/3}$ where $C(\rho)$ is a constant that depends only on ρ by virtue of (4.18).

To summarize, we have shown

$$\begin{aligned} &\mathbb{P}^\rho\{\exists z \in \mathcal{D} : \mathbf{Z}^{-\lfloor rN^{2/3} \rfloor e_1 \rightarrow z} = \lfloor rN^{2/3} \rfloor + t_0\} \\ &\leq \mathbb{P}(A^c) + \mathbb{P}^\rho(\{\exists z \in \mathcal{D} : \mathbf{Z}^{-\lfloor rN^{2/3} \rfloor e_1 \rightarrow z} = \lfloor rN^{2/3} \rfloor + t_0\} \cap A) \\ &\leq e^{-Cr^3} + (C(\rho)rN^{-1/3})^2. \end{aligned}$$

With a union bound over t_0 ,

$$\begin{aligned} &\mathbb{P}^\rho\{\exists z \in \mathcal{D} : \lfloor rN^{2/3} \rfloor - \delta N^{2/3} \leq \mathbf{Z}^{-\lfloor rN^{2/3} \rfloor e_1 \rightarrow z} \leq \lfloor rN^{2/3} \rfloor + \delta N^{2/3}\} \\ &\leq \mathbb{P}(A^c) + \mathbb{P}^\rho(\{\exists z \in \mathcal{D} : \lfloor rN^{2/3} \rfloor - \delta N^{2/3} \leq \mathbf{Z}^{-\lfloor rN^{2/3} \rfloor e_1 \rightarrow z} \leq \lfloor rN^{2/3} \rfloor + \delta N^{2/3}\} \cap A) \\ &\leq e^{-Cr^3} + (2\delta N^{2/3})(C(\rho)rN^{-1/3})^2 \\ &= e^{-Cr^3} + C(\rho)2\delta r^2. \end{aligned}$$

Letting $r = (C^{-1}|\log \delta|)^{1/3}$, this gives the desired upper bound $C(\rho)\delta|\log \delta|^{2/3}$ with a new constant $C(\rho)$. This completes the proof for the dark region \mathcal{D} of Figure 4.6.

For geodesics that enter \mathcal{L}^+ we use monotonicity that comes from uniqueness of finite geodesics:

$$\begin{aligned} &\mathbb{P}^\rho\{\exists v \in \mathcal{L}^+ : 1 \leq \mathbf{Z}^{0 \rightarrow v} \leq \delta N^{2/3}\} \leq \mathbb{P}^\rho\{\exists v \in \mathcal{L}^+ : \mathbf{Z}^{0 \rightarrow v} \geq 1\} \\ &\leq \mathbb{P}^\rho\{\mathbf{Z}^{0 \rightarrow w_N^+} \geq 1\} \leq e^{-Cr^3} = \delta. \end{aligned}$$

The last inequality comes from bound (3.8) from Corollary 3.6.

For geodesics that enter \mathcal{L}^- , this follows from Lemma 4.3. First, from the uniqueness of finite geodesics, it suffices to look at the point w_N^- since

$$\mathbb{P}^\rho\{\exists v \in \mathcal{L}^- : 1 \leq \mathbf{Z}^{0 \rightarrow v} \leq \delta N^{2/3}\} \leq \mathbb{P}^\rho\{\mathbf{Z}^{0 \rightarrow w_N^-} \leq \delta N^{2/3}\}.$$

Trace back a $(-\xi[\rho])$ -directed ray from the point w_N^- . Up to a ρ -dependent constant, this ray crosses the x -axis at $\lfloor \frac{(1-\rho)^2}{\rho^2}qrN^{2/3} \rfloor e_1$ (the white dot in Figure 4.10). Decrease δ_0 further if necessary so that $\delta < \delta_0 \leq \frac{(1-\rho)^2}{2\rho^2}qr$. Then the distance between the black and white dots in Figure 4.10 is at least $\frac{(1-\rho)^2}{2\rho^2}qrN^{2/3}$.

Let h be the positive integer such that $(\lfloor \delta r N^{2/3} \rfloor, -h)$ is the closest lattice point to the $(-\xi[\rho])$ -directed ray from w_N^- . Then, $h \geq \frac{1}{2}qrN^{2/3}$. From Lemma 3.1, whenever $\mathbf{Z}^{0 \rightarrow w_N^-} \leq \delta N^{2/3}$ (gray dotted line), then $\mathbf{Z}(\lfloor \delta N^{2/3} \rfloor, -h) \rightarrow w_N^- < -h$ (black dotted line). Theorem 3.5 bounds this probability by e^{-Cr^3} . This completes the proof of Theorem 4.5. \square

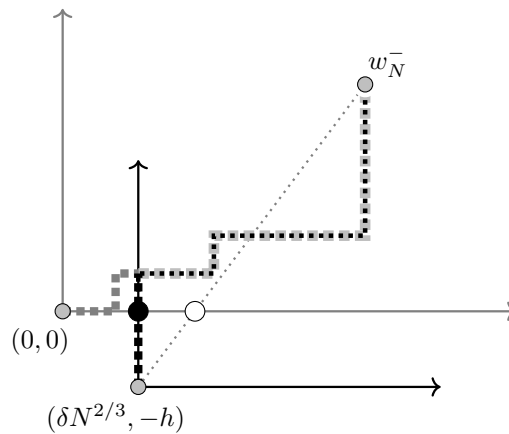


Figure 4.10: From Lemma 4.3, if $Z^0 \rightarrow w_N^- \leq \delta N^{2/3}$ (gray dotted line), then $Z^{\lfloor \delta N^{2/3} \rfloor, -h} \rightarrow w_N^- \leq -h$ (black dotted line).

5 Dual geodesics and proofs of the main theorems

The main theorems from Section 2 are proved by applying the exit time bounds of Section 4 to dual geodesics that live on the dual lattice. First define south and west directed semi-infinite paths (superscript sw) in terms of the Busemann functions from Theorem 3.7:

$$\begin{aligned}
 \mathbf{b}_0^{\text{sw},\rho,x} &= x, \quad \text{and for } k \geq 0 \\
 \mathbf{b}_{k+1}^{\text{sw},\rho,x} &= \begin{cases} \mathbf{b}_k^{\text{sw},\rho,x} - e_1, & \text{if } B_{\mathbf{b}_k^{\text{sw},\rho,x} - e_1}^\rho, \mathbf{b}_k^{\text{sw},\rho,x} \leq B_{\mathbf{b}_k^{\text{sw},\rho,x} - e_2}^\rho, \mathbf{b}_k^{\text{sw},\rho,x} \\ \mathbf{b}_k^{\text{sw},\rho,x} - e_2, & \text{if } B_{\mathbf{b}_k^{\text{sw},\rho,x} - e_2}^\rho, \mathbf{b}_k^{\text{sw},\rho,x} < B_{\mathbf{b}_k^{\text{sw},\rho,x} - e_1}^\rho, \mathbf{b}_k^{\text{sw},\rho,x}. \end{cases} \quad (5.1)
 \end{aligned}$$

Recall the dual weights $\{\check{\omega}_x^\rho = B_{x-e_1,x}^\rho \wedge B_{x-e_2,x}^\rho\}_{x \in \mathbb{Z}^2}$ introduced in part (iii) of Theorem 3.7.

Let $e^* = \frac{1}{2}(e_1 + e_2) = (\frac{1}{2}, \frac{1}{2})$ denote the shift between the lattice \mathbb{Z}^2 and its dual $\mathbb{Z}^{2*} = \mathbb{Z}^2 + e^*$. Shift the dual weights to the dual lattice by defining $\omega_z^* = \check{\omega}_{z+e^*}^\rho$ for $z \in \mathbb{Z}^{2*}$. By Theorem 3.7(iii) these weights are i.i.d. $\text{Exp}(1)$. The LPP process for these weights is defined as in (2.1):

$$G_{x,y}^* = \max_{z \in \Pi^{x,y}} \sum_{k=0}^{|y-x|_1} \omega_{z_k}^*. \quad (5.2)$$

Shift the southwest paths to the dual lattice by defining

$$\mathbf{b}_k^{*,\rho,z} = \mathbf{b}_k^{\text{sw},\rho,z+e^*} - e^* \quad \text{for } z \in \mathbb{Z}^{2*} \text{ and } k \geq 0.$$

These definitions reproduce on the dual lattice the semi-infinite geodesic setting described in Section 3.3, with reflected lattice directions. This is captured in the next theorem that summarizes the development from Section 4.2 of [28].

Theorem 5.1. Fix $\rho \in (0, 1)$. Then the following hold almost surely.

- (i) For each $z \in \mathbb{Z}^{2*}$, the path $\mathbf{b}^{*,\rho,z}$ is the unique $(-\xi[\rho])$ -directed semi-infinite geodesic from z in the LPP process (5.2). Precisely,

$$\lim_{n \rightarrow \infty} \frac{\mathbf{b}_n^{*,\rho,z}}{n} = -\xi[\rho] \quad \text{and} \quad \forall k < l \text{ in } \mathbb{Z}_{\geq 0} : G_{\mathbf{b}_l^{*,\rho,z}, \mathbf{b}_k^{*,\rho,z}}^* = \sum_{i=k}^l \omega_{\mathbf{b}_i^{*,\rho,z}}^*.$$

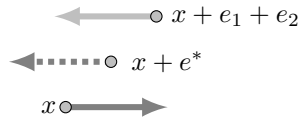


Figure 5.1: The equivalent events $\mathbf{b}_1^{\rho,x} = x + e_1$ (dark gray arrow), $\mathbf{b}_1^{\text{sw},\rho,x+e_1+e_2} = x + e_2$ (light gray arrow), and $\mathbf{b}_k^{*,\rho,x+e^*} = x + e^* - e_1$ (dotted arrow). The dark gray and dotted arrows never cross.

(ii) *The semi-infinite geodesics and the dual semi-infinite geodesics are equal in distribution, modulo the e^* -shift and lattice reflection: $\{\mathbf{b}^{*,\rho,z}\}_{z \in \mathbb{Z}^{*2}} \stackrel{d}{=} \{-e^* - \mathbf{b}^{\rho,-(z+e^*)}\}_{z \in \mathbb{Z}^{*2}}$.*

(iii) *The collections of paths $\{\mathbf{b}^{\rho,z}\}_{z \in \mathbb{Z}^2}$ and $\{\mathbf{b}^{*,\rho,z}\}_{z \in \mathbb{Z}^{*2}}$ almost surely never cross each other.*

Part (ii), the distributional equality of the tree of directed geodesics and the dual, was first proved in [24]. The non-crossing property of part (iii) can be seen from a simple picture. The additivity of the Busemann functions gives

$$B_{x,x+e_1}^\rho + B_{x+e_1,x+e_1+e_2}^\rho = B_{x,x+e_2}^\rho + B_{x+e_2,x+e_1+e_2}^\rho. \tag{5.3}$$

By (3.9) $\mathbf{b}_1^{\rho,x} = x + e_1$ if and only if $B_{x,x+e_1}^\rho \leq B_{x,x+e_2}^\rho$. By (5.3) this is equivalent to $B_{x+e_2,x+e_1+e_2}^\rho \leq B_{x+e_1,x+e_1+e_2}^\rho$ which is the same as $\mathbf{b}_1^{\text{sw},\rho,x+e_1+e_2} = x + e_2$, and this last is equivalent to $\mathbf{b}_k^{*,\rho,x+e^*} = x + e^* - e_1$. An analogous argument works for the e_2 step. The conclusion is that the increments of $\mathbf{b}^{\rho,\bullet}$ out of x and $\mathbf{b}^{*,\rho,\bullet}$ out of $x + e^*$ cannot cross. See Figure 5.1.

To connect the dual semi-infinite geodesics with ρ -geodesics, define a stationary LPP process $G_{-e^*,\bullet}^{*,\rho}$, exactly as in (3.4) with boundary weights on the south and east boundaries, but on the dual quadrant $-e^* + \mathbb{Z}_{\geq 0}^2$ based at $-e^*$. The boundary weights are defined by shifting Busemann function values to the dual lattice:

$$I_{-e^*+ke_1}^{*,\rho} = B_{(k-1)e_1,ke_1}^\rho \quad \text{and} \quad J_{-e^*+le_2}^{*,\rho} = B_{(l-1)e_1,le_1}^\rho.$$

The bulk weights are $\{\omega_x^* : x \in \mathbb{Z}^{*2}, x \geq e^*\}$.

Proposition 5.2. *For any $w \in e^* + \mathbb{Z}_{\geq 0}^2$ the following holds. The edges of the semi-infinite geodesic $\mathbf{b}^{*,\rho,w}$ that have at least one endpoint in $e^* + \mathbb{Z}_{\geq 0}^2$ are also edges of the geodesic of $G_{-e^*,w}^{*,\rho}$.*

Proposition 5.2, illustrated in Figure 5.2, is another version of Lemma 3.2. It is proved as Prop. 5.1 in [28] but without the shift to the dual lattice, so in terms of the southwest geodesics in (5.1) for the weights $\check{\omega}^\rho$.

We are ready to prove the main results.

Proof of Theorem 2.2. Referring to Figure 5.3, geodesics $\mathbf{b}^{\rho,(0, \lfloor \delta N^{2/3} \rfloor)}$ and $\mathbf{b}^{\rho,(\lfloor \delta N^{2/3} \rfloor, 0)}$ (gray dotted lines) coalesce outside $\llbracket 0, v_N \rrbracket$ if and only if some dual geodesic started outside of $\llbracket 0, v_N \rrbracket - e^*$ (black dotted line) enters the square $\llbracket (0, 0), (\lfloor \delta N^{2/3} \rfloor, \lfloor \delta N^{2/3} \rfloor) \rrbracket$. From Proposition 5.2, the restrictions of these dual geodesics are the ρ -geodesics of the stationary LPP process on $-e^* + \mathbb{Z}_{\geq 0}^2$ with Busemann boundary weights on the south and west. Consequently

$$\mathbb{P}\{\mathbf{z}^\rho(\lfloor \delta N^{2/3} \rfloor e_1, \lfloor \delta N^{2/3} \rfloor e_2) \notin \llbracket 0, v_N \rrbracket\} = \mathbb{P}^\rho\{\exists z \notin \llbracket 0, v_N \rrbracket : |\mathbf{Z}^0 \rightarrow z| \leq \delta N^{2/3}\}. \tag{5.4}$$

The bounds claimed in Theorem 2.2 follow from Theorems 4.4 and 4.5. \square

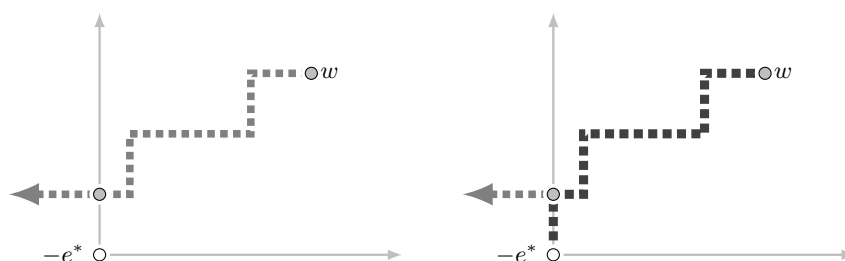


Figure 5.2: Illustration of Proposition 5.2. On the left the dual semi-infinite geodesic $\mathbf{b}^{*,\rho,w}$ (light dotted path). On the right the geodesic of $G_{-e^*,w}^{*,\rho}$ (dark dotted path). The two paths coincide in the bulk.

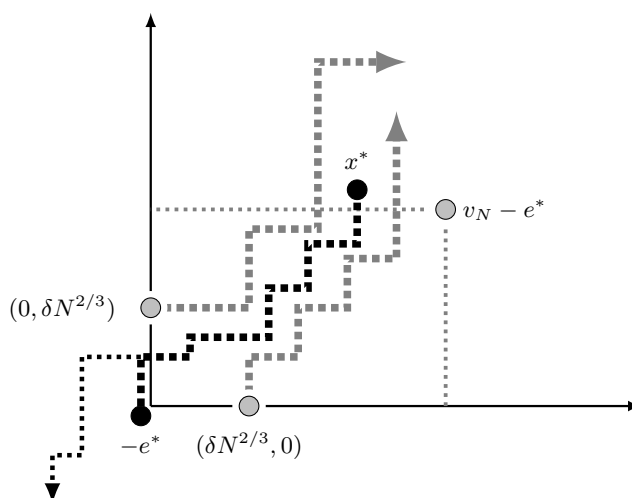


Figure 5.3: Geodesics $\mathbf{b}^{\rho,(\lfloor \delta N^{2/3} \rfloor, 0)}$ and $\mathbf{b}^{\rho,(0, \lfloor \delta N^{2/3} \rfloor)}$ (gray dotted lines) coalesce outside $\llbracket 0, v_N \rrbracket$. Equivalently, some dual point x^* outside of $\llbracket 0, v_N \rrbracket - e^*$ sends a dual geodesic (black dotted line) into the rectangle $\llbracket (0, 0), (\lfloor \delta N^{2/3} \rfloor, \lfloor \delta N^{2/3} \rfloor) \rrbracket$.

Proof of Theorem 2.3. Referring to Figure 5.4, geodesics $\mathbf{b}^{\rho,(0, \lfloor rN^{2/3} \rfloor)}$ and $\mathbf{b}^{\rho,(\lfloor rN^{2/3} \rfloor, 0)}$ (gray dotted lines) coalesce inside $\llbracket 0, v_N \rrbracket$ if and only if every dual geodesic started from the north and east boundaries of $\llbracket -e^*, v_N + e^* \rrbracket$ (black dotted lines) avoids the square $\llbracket (0, 0), (\lfloor rN^{2/3} \rfloor, \lfloor rN^{2/3} \rfloor) \rrbracket$. From Proposition 5.2, the restrictions of these dual geodesics are the ρ -geodesics of the stationary LPP process on $-e^* + \mathbb{Z}_{\geq 0}^2$ with Busemann boundary weights on the south and west,

$$\mathbb{P}\{\mathbf{z}^\rho(\lfloor rN^{2/3} \rfloor e_1, \lfloor rN^{2/3} \rfloor e_2) \in \llbracket 0, v_N \rrbracket\} = \mathbb{P}^\rho\{\forall z \notin \llbracket 0, v_N \rrbracket : |\mathbf{Z}^{0 \rightarrow z}| \geq rN^{2/3}\}. \quad (5.5)$$

The lower bound claimed in Theorem 2.3 follows from Theorem 4.1. The claimed upper bound is a trivial weakening of Theorem 3.5. \square

Proof of Corollary 2.4. From the duality, it suffices to show

- (i) $\mathbb{P}^\rho\{\exists z \text{ outside } \llbracket 0, v_N \rrbracket \text{ such that } 1 \leq \mathbf{Z}^{0 \rightarrow z} \leq \delta N^{2/3}\} \geq C_1 \delta;$
- (ii) $\mathbb{P}^\rho\{\exists z \text{ outside } \llbracket 0, v_N \rrbracket \text{ such that } 1 \leq \mathbf{Z}^{0 \rightarrow z} \leq rN^{2/3}\} \geq 1 - e^{-C_2 r^3}.$

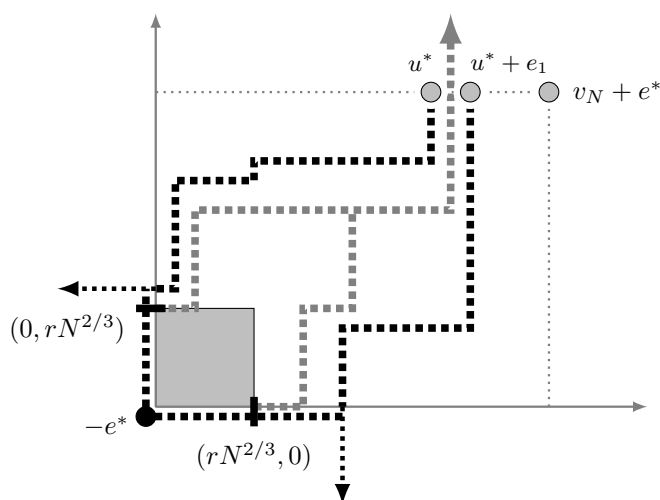


Figure 5.4: None of the the ρ -geodesics will enter the gray square because they are bounded away by the two dual geodesics (black dotted lines) drawn above.

We establish (ii) from the special case

$$\mathbb{P}^\rho \left\{ 1 \leq \mathbf{Z}^{0 \rightarrow v_N + \lfloor \frac{1}{10} r N^{2/3} \rfloor e_1} \leq r N^{2/3} \right\} \geq 1 - e^{-C_2 r^2}. \tag{5.6}$$

Furthermore, from (5.6) the proof of Theorem 4.4 can be adapted to prove (i), by partitioning $[0, rN^{2/3}]$ into intervals of size $\leq \delta r N^{2/3}$ and repeating the argument.

Inequality (5.6) comes from the estimates

$$\mathbb{P}^\rho \left\{ \mathbf{Z}^{0 \rightarrow v_N + \lfloor \frac{1}{10} r N^{2/3} \rfloor e_1} \leq -1 \right\} \leq e^{-C r^3} \tag{5.7}$$

$$\mathbb{P}^\rho \left\{ \mathbf{Z}^{0 \rightarrow v_N + \lfloor \frac{1}{10} r N^{2/3} \rfloor e_1} > r N^{2/3} \right\} \leq e^{-C r^3}. \tag{5.8}$$

Inequality (5.7) is bound (3.7) of Corollary 3.6. For (5.8), apply Lemma 3.4 to the process $G_{z, \cdot}^{(0), \rho}$ with the new base point $z = \lfloor \frac{1}{10} r N^{2/3} \rfloor e_1$, and then Theorem 3.5:

$$\mathbb{P}^\rho \left\{ \mathbf{Z}^{0 \rightarrow v_N + \lfloor \frac{1}{10} r N^{2/3} \rfloor e_1} \geq r N^{2/3} \right\} \leq \mathbb{P}^\rho \left\{ \mathbf{Z}^{0 \rightarrow v_N} \geq \frac{9}{10} r N^{2/3} \right\} \leq e^{-C r^3}. \quad \square$$

Proof of Theorem 2.8. If the semi-infinite geodesic $\mathbf{b}^{\rho, (0,0)}$ enters the interior of the square $\llbracket v_N - (\delta N^{2/3}, \delta N^{2/3}), v_N \rrbracket$ as shown in Figure 5.5, we obtain a ρ -geodesic from Proposition 5.2 whose exit time satisfies $|\mathbf{Z}^{NE,0 \rightarrow v_N}| \leq \delta N^{2/3}$. Applying the exit time estimate Theorem 4.5 finishes the proof. \square

A Appendix

Below is the random walk estimate for the proof of Theorem 4.5. It is proved as Lemma C.1 in Appendix C of [2].

Lemma A.1. *Let $\alpha > \beta > 0$. Let $S_n = \sum_{k=1}^n Z_k$ be a random walk with step distribution $Z_k \sim \text{Exp}(\alpha) - \text{Exp}(\beta)$ (difference of independent exponentials). Then there is an absolute constant C independent of all the parameters such that for $n \in \mathbb{Z}_{>0}$,*

$$\mathbb{P}(S_1 < 0, S_2 < 0, \dots, S_n < 0) \leq \frac{C}{\sqrt{n}} \left(1 - \frac{(\alpha - \beta)^2}{(\alpha + \beta)^2} \right)^n + \frac{\alpha - \beta}{\alpha}. \tag{A.1}$$

References

- [1] Gideon Amir, Omer Angel, and Benedek Valkó, *The TASEP speed process*, Ann. Probab. **39** (2011), no. 4, 1205–1242. MR-2857238
- [2] Márton Balázs, Ofer Busani, and Timo Seppäläinen, *Non-existence of bi-infinite geodesics in the exponential corner growth model*, 2019, arXiv:1909.06883. MR-4116707
- [3] Márton Balázs, Ofer Busani, and Timo Seppäläinen, *Local stationarity of exponential last passage percolation*, 2020, arXiv:1909.06883.
- [4] Márton Balázs, Eric Cator, and Timo Seppäläinen, *Cube root fluctuations for the corner growth model associated to the exclusion process*, Electron. J. Probab. **11** (2006), no. 42, 1094–1132 (electronic). MR-2268539
- [5] Márton Balázs, Júlia Komjáthy, and Timo Seppäläinen, *Microscopic concavity and fluctuation bounds in a class of deposition processes*, Ann. Inst. Henri Poincaré Probab. Stat. **48** (2012), no. 1, 151–187. MR-2919202
- [6] Márton Balázs and Timo Seppäläinen, *Order of current variance and diffusivity in the asymmetric simple exclusion process*, Ann. of Math. (2) **171** (2010), no. 2, 1237–1265. MR-2630064
- [7] Riddhipratim Basu, Sourav Sarkar, and Allan Sly, *Coalescence of geodesics in exactly solvable models of last passage percolation*, J. Math. Phys. **60** (2019), no. 9, 093301, 22. MR-4002528
- [8] Manan Bhatia, *Moderate deviation and exit time estimates for stationary last passage percolation*, 2020, arXiv:2004.12987.
- [9] Eric Cator and Piet Groeneboom, *Second class particles and cube root asymptotics for Hammersley’s process*, Ann. Probab. **34** (2006), no. 4, 1273–1295. MR-2257647
- [10] Hans Chaumont and Christian Noack, *Characterizing stationary 1 + 1 dimensional lattice polymer models*, Electron. J. Probab. **23** (2018), Paper No. 38, 19. MR-3806406
- [11] Ivan Corwin, *The Kardar-Parisi-Zhang equation and universality class*, Random Matrices Theory Appl. **1** (2012), no. 1, 1130001, 76. MR-2930377
- [12] David Coupier, *Multiple geodesics with the same direction*, Electron. Commun. Probab. **16** (2011), 517–527. MR-2836758
- [13] Murray Eden, *A two-dimensional growth process*, Proc. 4th Berkeley Sympos. Math. Statist. and Probab., Vol. IV, Univ. California Press, Berkeley, Calif., 1961, pp. 223–239. MR-0136460
- [14] Elnur Emrah, Chris Janjigian, and Timo Seppäläinen, *Right-tail moderate deviations in the exponential last-passage percolation*, 2020, arXiv:2004.04285.
- [15] Wai-Tong Louis Fan and Timo Seppäläinen, *Joint distribution of Busemann functions in the exactly solvable corner growth model*, 2018, arXiv:1808.09069.
- [16] Pablo A. Ferrari and Leandro P. R. Pimentel, *Competition interfaces and second class particles*, Ann. Probab. **33** (2005), no. 4, 1235–1254. MR-2150188
- [17] Nicos Georgiou, Firas Rassoul-Agha, and Timo Seppäläinen, *Stationary cocycles and Busemann functions for the corner growth model*, Probab. Theory Related Fields **169** (2017), no. 1-2, 177–222. MR-3704768
- [18] J. M. Hammersley and D. J. A. Welsh, *First-passage percolation, subadditive processes, stochastic networks, and generalized renewal theory*, Proc. Internat. Res. Semin., Statist. Lab., Univ. California, Berkeley, Calif, Springer-Verlag, New York, 1965, pp. 61–110. MR-0198576
- [19] C. Douglas Howard and Charles M. Newman, *Euclidean models of first-passage percolation*, Probab. Theory Related Fields **108** (1997), no. 2, 153–170. MR-1452554
- [20] C. Douglas Howard and Charles M. Newman, *Geodesics and spanning trees for Euclidean first-passage percolation*, Ann. Probab. **29** (2001), no. 2, 577–623. MR-1849171
- [21] Christopher Janjigian, Firas Rassoul-Agha, and Timo Seppäläinen, *Geometry of geodesics through Busemann measures in directed last-passage percolation*, 2019, arXiv:1908.09040. MR-3838897
- [22] Cristina Licea and Charles M. Newman, *Geodesics in two-dimensional first-passage percolation*, Ann. Probab. **24** (1996), no. 1, 399–410. MR-1387641

- [23] Charles M. Newman, *A surface view of first-passage percolation*, Proceedings of the International Congress of Mathematicians, Vol. 1, 2 (Zürich, 1994), Birkhäuser, Basel, 1995, pp. 1017–1023. MR-1404001
- [24] Leandro P. R. Pimentel, *Duality between coalescence times and exit points in last-passage percolation models*, Ann. Probab. **44** (2016), no. 5, 3187–3206. MR-3551194
- [25] Jeremy Quastel, *Introduction to KPZ*, Current developments in mathematics, 2011, Int. Press, Somerville, MA, 2012, pp. 125–194. MR-3098078
- [26] Timo Seppäläinen, *Scaling for a one-dimensional directed polymer with boundary conditions*, Ann. Probab. **40** (2012), no. 1, 19–73, Corrected version available at arXiv:0911.2446. MR-2917766
- [27] Timo Seppäläinen, *The corner growth model with exponential weights*, Random growth models, Proc. Sympos. Appl. Math., vol. 75, Amer. Math. Soc., Providence, RI, 2018, arXiv:1709.05771, pp. 133–201. MR-3838898
- [28] Timo Seppäläinen, *Existence, uniqueness and coalescence of directed planar geodesics: proof via the increment-stationary growth process*, 2018, To appear in Ann. Inst. Henri Poincaré Probab. Stat., arXiv:1812.02689. MR-4116707
- [29] Mario V. Wüthrich, *Asymptotic behaviour of semi-infinite geodesics for maximal increasing subsequences in the plane*, In and out of equilibrium (Mambucaba, 2000), Progr. Probab., vol. 51, Birkhäuser Boston, Boston, MA, 2002, pp. 205–226. MR-1901954

Acknowledgments. The authors gratefully thank the anonymous referee for his/her suggestions about improving the exposition of this paper.

Electronic Journal of Probability

Electronic Communications in Probability

Advantages of publishing in EJP-ECP

- Very high standards
- Free for authors, free for readers
- Quick publication (no backlog)
- Secure publication (LOCKSS¹)
- Easy interface (EJMS²)

Economical model of EJP-ECP

- Non profit, sponsored by IMS³, BS⁴, ProjectEuclid⁵
- Purely electronic

Help keep the journal free and vigorous

- Donate to the IMS open access fund⁶ (click here to donate!)
- Submit your best articles to EJP-ECP
- Choose EJP-ECP over for-profit journals

¹LOCKSS: Lots of Copies Keep Stuff Safe <http://www.lockss.org/>

²EJMS: Electronic Journal Management System <http://www.vtex.lt/en/ejms.html>

³IMS: Institute of Mathematical Statistics <http://www.imstat.org/>

⁴BS: Bernoulli Society <http://www.bernoulli-society.org/>

⁵Project Euclid: <https://projecteuclid.org/>

⁶IMS Open Access Fund: <http://www.imstat.org/publications/open.htm>